POSITIONING CONTROL OF DIRECT DRIVE SYSTEM

CHRISTINE TIONG SHI MING

BACHELOR OF ELECTRICAL ENGINEERING

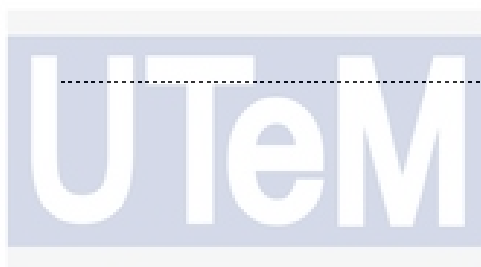# UNIVERSITI TEKNIKAL MALAYSIA MELAKA

"I hereby declared that I have read through this report entitled "Positioning Control of Direct Drive System" and found that it complies the partial fulfilment for awarding the degree of Bachelor of Electrical Engineering"

Signature   :   ....

Supervisor's Name   :   Assoc Prof. Dr. Chong Shin Horng

Date   :   ....

POSITIONING CONTROL OF DIRECT DRIVE SYSTEM

CHRISTINE TIONG SHI MING

A report submitted in partial fulfilment of the requirements for the degree of
Bachelor of Electrical Engineering
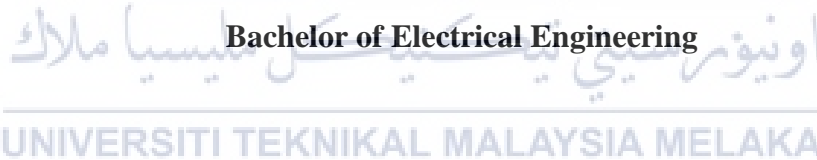
Faculty of Electrical Engineering
UNIVERSITI TEKNIKAL MALAYSIA MELAKA

2018

I declare that this report entitled "Positioning Control of Direct Drive System" is the result of my own research except as cited in the references. This report has not been accepted for any degree and is not concurrently submitted in candidature of any other degree.

Signature   :   ....

Name   :   Christine Tiong Shi Ming

Date   :   26/05/2018

To my beloved father and mother

ACKNOWLEDGEMENT

First and foremost, I would like to thank to Almighty God for giving me the strength, ability and opportunity to undergo this project satisfactorily. With His blessings, I could preserve in a good health, peace and joy during my Final Year Project II (FYP II). Next, I would like to take this opportunity to express my sincere acknowledgement to my supervisor, Assoc Prof. Dr. Chong Shin Horng from the Faculty of Electrical Engineering (FKE) in Universiti Teknikal Malaysia Melaka (UTeM) for her essential supervision, support and encouragement towards the completion of this thesis. Special thanks to all my friends, my beloved mother and siblings for their moral support in completing this final year project. Lastly thank you to everyone who had been associated to the crucial parts of realization of this project.
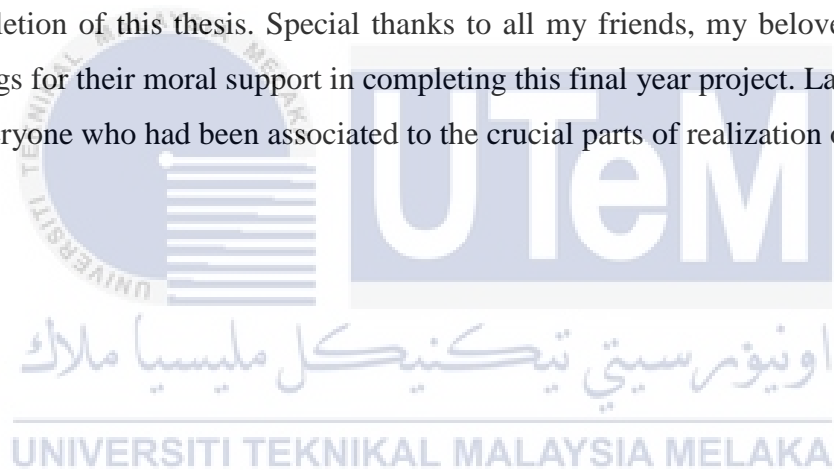
ABSTRACT

This project discusses the positioning control of a direct drive system. The direct drive system is driven using an ironless permanent-magnet linear motor (IPMLM) to directly drive the mechanism in a linear motion. Direct drive system is an advanced technology that has been widely used in extensive area of high-speed applications due to its simple structure, high accuracy and high speed. However, it is highly sensitive towards the disturbances and parameter variation affected by the elimination of the mechanical transmission elements. The existing Continuous Motion Nominal Characteristics Trajectory Following (CM-NCTF) controller has showed its promising positioning performance in PTP and tracking motions, however, its performance is deteriorated, demonstrates a slow-motion in high frequency motion of 5 Hz. The main objective of the project is to design a fast positioning control for a direct drive system to achieve a fast response at point-to-point and tracking motions at high frequency simultaneously. As a solution, a feedforward compensator is incorporated to the CM-NCTF controller in order to improve the following characteristic of the control system, and thus perform smaller tracking error. The positioning performance of the controller is validated experimentally in PTP and in tracking motions.

ABSTRAK

Projek ini membincangkan kawalan kedudukan sistem pemanduan langsung. Sistem pemacu langsung dipandu dengan motor bersifat linear tanpa magnet (IPMLM) untuk terus memacu mekanisme dalam gerakan linear. Sistem pemacu langsung adalah teknologi canggih yang telah digunakan secara luas dalam aplikasi yang memerlukan kelajuan yang tinggi kerana strukturnya mudah, sama sekali dengan tinggi prestasinya dalam sifat ketepatan dan kelajuan. Walau bagaimanapun, system ini sangat sensitif terhadap gangguan dan variasi parameter yang terjejas oleh penghapusan elemen penghantaran mekanikal. Pengawal Ciri-ciri Trajektori Berterusan (CM-NCTF) telah menunjukkan prestatsi kedudukannya yang menjanjikan di PTP dan gerakan pengesanan, tetapi prestasinya telah merosot dan menunjukkan gerakan yang perlahan dalam frekuensi yang tinggi dengan 5 Hz. Tujuan utama projek ini adalah untuk merekabentuk kawalan kedudukan dengan pantas oleh sistem pemacu langsung untuk mencapai tindak balas pantas pada gerakan PTP dan untuk melaksanakan gerakan penjejakan tinggi pada frekuensi tinggi dengan serentak. Untuk meyelesaikan masalah ini, pemampan feedforward dimasukkan kepada pengawal CM-NCTF untuk memperbaiki ciri-ciri berikut dalam sistem kawalan, dan dengan itu menunjukkan ralat yang kecil dalm gerakan pengesanan. Prestasi kedudukan pengawal disahkan secara cuba dari segi pergerakan PTP dan pengesanan.

TABLE OF CONTENTS

LIST OF TABLES

LIST OF FIGURES

FIGURE	TITLE	PAGE

UNIVERSITI TEKNIKAL MALAYSIA MELAKA

LIST OF ABBREVIATIONS

1-DOF	-	One-degree-of-freedom
2-DOF	-	Two-degree-of-freedom
%OS	-	Percentage overshoot
a	-	Acceleration
AC	-	Alternating current
ANN	-	Artificial neural network
AR-CM NCTF	-	Acceleration Reference Continuous Motion Nominal Characteristics Following
b	-	Friction coefficient
β	-	Inclination (slope)
BSD	-	Ball screw drive
CM-NCTF	-	Continuous Motion Nominal Characteristics Trajectory Following
CP	-	continuous path
DOB	-	disturbance observer-based
E_{max}/ e_{max}	-	Maximum error
e_{rms}	-	root-mean-square error
E_{ss}/ SSE	-	Steady-state error
FF	-	Feedforward
F_{fri}	-	Equivalent friction force generated
F_i	-	Inertial force
FLC	-	Fuzzy logic controller
FNNC	-	Fuzzy-neural-network controller
F_{thrust}	-	Thrust force
I_a	-	Current applied to the system
ILC	-	Iterative Learning Control
IPMLM	-	Ironless permanent-magnet linear motor
K_a	-	Voltage-to-current gain

K_{ff}	-	Velocity feedforward gain
K_i	-	Integral gain
K_m	-	Motor force constant
K_p	-	Proportional gain
LDD	-	Linear direct drive
LQR	-	Linear quadratic regulator
M	-	Mass of the load
NCT	-	Nominal characteristics trajectory
NCTF	-	Nominal characteristics trajectory following
PC	-	Personal compute
PD	-	Proportional derivative
PDDO	-	Proportional derivative with disturbance observer
PFPID	-	Predictive feedforward PID
PI	-	Proportional-integral
PID	-	Proportional-integral-derivative
PMLM	-	Permanent-magnet linear motor
PTOS	-	Proximate time-optimal servomechanism
PTP	-	Point-to-point
RPD	-	Rack and pinion drives
SMC	-	Sliding mode controller
T_d/t_r	-	Duty cycle/time width
t_f	-	Total time of motion
t_r/T_{rise}	-	Rise time
T_s	-	Sampling time
t_s/T_{settle}	-	Settling time
u/u_r	-	Voltage input to the motor
UC	-	Updated control
UR	-	Updated reference
v	-	Velocity
x	-	Position of the mover
x_f	-	Final displacement
$\dot{x}_r$	-	Feedforward signal
ZPETC	-	Zero-Phase-Error-Tracking Controller

CHAPTER 1

INTRODUCTION

1.1   Background

Unlike indirect drive system composed of rotary motor with ball screws, direct drive system consists of a mechanical actuator that directly drives the mechanism in a linear motion without mechanical transmission elements, such as gears and screws [1]. The mechanical transmission elements have physically limit the accuracy of the system by introducing backlash and high compact frictions. By eliminating the use of mechanical transmission elements, direct drive system performs a high speed and high accuracy positioning systems. Nowadays, direct drive system has rapidly gained its popularity among industrial applications such as machine tools, semiconductor manufacturing equipment, precision milling, automatic inspection machines and aerospace manufacturing [2].

Linear motor drive system is a kind of direct drive system, thus permanent-magnet linear motor (PMLM) can serve as direct drive motor [3]. The PMLM has promised a lot of advantages, which are the high positioning precision and accuracy due to its simplicity structure and achievable high-force density [4]. The force is applied directly to the mechanism without power transmission to another part of elements, known as mechanical transmission elements. However, as compared with the indirect drive motor that contains transmission elements, PMLM are highly sensitive to the disturbances and the variation of parameters [5]. The friction (Coulomb, viscous and stiction) and the force ripples (detent and reluctance forces) are the major nonlinearities arising from deficiencies in the basic components [6]. These problems will directly affect the performance of the system response. In order to optimize the positioning performance of PMLM, the positioning control of the system is essential

to perform typical requirements of the industrial applications with high-speed, high precision and fast response. This control system is used to offset any disturbances arise, as the system may alter the variables like velocity and displacement [7]. To minimize these problems, there are lots of efforts have been devoted to the control system.

There are many controllers have been proposed, such as proportional-integral-derivative (PID) controller, disturbance observer (DOB), sliding mode controller (SMC), fuzzy logic controller (FLC), linear quadratic controller, adaptive observer and so on. The conventional PID controller is widely used in industrial application due to its simplicity and good motion performance. However, it has limitation performance towards high demand for fast response with no or small overshoot [8]. The advanced controllers such as SMC and DOB has less sensitivity to the disturbance and parameter variations to achieve robustness and high performance of the system. But, these model-based controllers require the exact model and the parameter identification of the mechanism that might require a long-time consumption and the sufficient knowledge of control system theory on design process [9, 10]. After then, an intelligent controller such as FLC has been designed by several researchers [8, 11]. It does not require an exact model and parameter identification. Yet, the design process is complex due to its unsystematic approaches and high knowledge needed for the accurate tuning of FLC [12]. Therefore, as a practical solution, a Continuous Motion Nominal Characteristics Trajectory Following (CM-NCTF) controller has been proposed to solve these problems. CM-NCTF controller is a practical controller which is simple to design and it does not require an exact model and parameter identification of a mechanism [13].

In this project, an ironless permanent-magnet linear motor (IPMLM) is used to clarify the usefulness of the improved CM-NCTF control. The main aim of this project is to design a fast positioning controller for a direct drive system to optimize the positioning performance in high frequency. The performance of the controller will be validated and examined in various motion, such as point-to-point (PTP) and tracking motion.

1.2   Problem Statement

Mechanical systems have evolved from the screw transmission to the linear motor driven. Compared to indirect drive system, direct drive systems offer several advantages, and it can achieve higher speed and higher accuracy of position than indirect drive system like ball screw mechanism, without other power transmissions to the multiple component parts. However, direct drive system is highly sensitive to the disturbance and parameter variation. As both friction force and cutting force are directly acting on the motor, these disturbances could reduce the overall tracking performance, then the efficient control strategies are critical in machine tool direct drive application. Today, a high speed with high precision of motion control system is requested in many industrial applications to improve their qualities and production performances. Increasing the positioning speed and acceleration of the machine tool, decreasing in the non-cutting times, increasing in machine productivity. There are different controllers had been designed to improve the performance of the system.

In [14], the CM-NCTF controller has achieved a significant high tracking performance in different sinusoidal input signals and different frequencies, as compared to PTOS controller. As the frequency is increased at a same amplitude, or the amplitude of the reference input is increased at the same frequency, the maximum tracking error of the system is increased too. With amplitude input signal of 1 mm, the maximum tracking error of CM-NCTF controller is 89.8%, 88.7%, 90.6% and 95.5% smaller than of PTOS controller at 0.1 Hz, 1 Hz, 3 Hz and 5 Hz respectively. As observed in the result, CM-NCTF demonstrates small tracking error with only 1.7% in slow motion of 0.1 Hz and small working range of 0.1 mm. Therefore, the CM-NCTF controller shows its effectiveness on positioning performance in tracking motion. However, the maximum tracking error of the CM-NCTF controller is getting higher as the frequency increase. The maximum tracking error at amplitude of 5 mm is increased around 4 times from the frequency of 3 Hz increased to 5 Hz. Besides, at high frequency of 5 Hz, the maximum tracking error is 50 times higher than sensor (encoder) resolution, at 1 mm and 5 mm. Thus, CM-NCTF controller has demonstrated low tracking performance especially at high frequency motion.

As discussed in [14], the CM-NCTF controller does not show any steady-state error and overshoot in every different step input signals in point-to-point motion.

Therefore, the CM-NCTF controller is proved to be able to achieve a precise positioning performance. However, as compared to PTOS controller, the CM-NCTF control has shown slightly slow rise time and settling time at the large step input signal of 10 mm and 50 mm. From the results, the rise time of CM-NCTF controller is 1.6 times and 2.5 times slower than the PTOS controller, whereas the settling time of the CM-NCTF controller is 1.4 times and 2.3 times slower than the PTOS controller, at 10 mm and 50 mm respectively. The small control signal of the system leads to the slow response of the system. A feedforward element is to be assumed, in control theory, to increase the control signal, and simultaneously to fast the response of the system without any affect to the stability of the system. Therefore, in this paper, an additional feedforward compensator added to CM-NCTF controller is proposed to validate the PTP and tracking motion performance of the system for high frequency 5 Hz.

1.3 Objectives

The main objectives of the project are:

i. To design a fast positioning controller for a direct drive system;

ii. To validate the positioning performance of the control system in point-to-point and tracking motions in high frequency.

1.4 Scopes

The scopes of the project are:

i. The direct drive system used in this experiment is an ironless permanent-magnet linear motor (IPMLM).

ii. The IPMLM has a working range of ±100 mm.

iii. AC motor driver will produce 0.128 A for each corresponding voltage applied to drive the motor.

iv. The voltage is limited within a maximum range of ± 10V.

v. The sampling frequency of the controller is set to 1 kHz.

vi. The resolution of linear encoder is 0.2 µm.

vii. The achievable velocity of the system is ± 500 mm/s.

CHAPTER 2

LITERATURE REVIEW

2.1 Control System

Control systems have widespread applications in industries applications, from steering ships and planes to guiding missiles and the space shuttle. There are two major configurations of control systems, which are open-loop control system and closed-loop control system. The performance of the control system is usually analysed in terms of transient response and steady-state response. Steady-state response determines the accuracy of the control system, while transient response affects the speed of the system [15].

Today, positioning control systems play a significant part in industrial applications such as machine tools, industrial robots, semiconductor manufacturing system, material handling systems, electric transportation, disk drives, rolling mills, printers, and so forth. The accuracy of the positioning system is required to achieve a better and higher performance on the machine. In general, motion control systems can be classified into three types, which are point-to-point (PTP), tracking and continuous path (CP) motions. These motions are generally used to evaluate the performance of the system. S.H. Chong and K. Sato stated that, it is required to have a controller with a simple structure, which is easy to design, fast response, less overshoot, high robustness performance and high accuracy and resolution [16].

Conventional PID controller is widely used due to its practical, simple and straightforward applications. PID controller consists of proportional, integral and derivative. The proportional-integral (PI) controller is used to improve the steady state response by reducing the steady-state error. The proportional-derivative (PD) controller is used to improve the transient response. PID controller is using tuning

technique to determine the gain to optimize the response. PID controller is reliable if it is properly tuned [17]. However, this controller encounters its limitation to reach higher precision performance and system robustness. To improve this controller, different advanced controllers were designed.

Sliding mode controller (SMC) provides a simple and systematic way to achieve robust control system. SMC implements a high-speed discontinuous switching operation [18]. SMC has less sensitivity to the disturbance and parameter variations, and even disturbance rejection. However, SMC suffers from chattering or vibrating that lead to the limitation of practical application. Vibrating leads to low control accuracy, high heat losses in power circuits, and high wear of moving mechanical parts [18]. It may also excite unmodeled high-frequency dynamics, which degrade the performance of the system [19].

Disturbance observer-based controller (DOB) can estimate a disturbance and reject the disturbance without affecting performance. A disturbance compensation method of disturbance observer (DOB) was proposed by Satoshi, et al. for direct drive motor [5]. DOB showed a precise and high-performance path tracing control and force control. In [20, 21], a proportional derivative (PD) with disturbance observer (PDDO) was proposed to compensate a direct drive system. PDDO showed its robustness against disturbance and parameter variation in direct drive system compared to PID controller. However, these controllers are model-based controllers, where the system performance is depending on the accuracy of the identified model and the parameters used [22]. Therefore, these advanced model-based controllers are complex design and time-consuming, results the unreliability applications in the industry.

Fuzzy logic and neural network techniques are extensively implement in machine tools applications. the fuzzy logic control (FLC) and artificial neural network (ANN) do not require a mathematical model of the system. Artificial neural network (ANN) offer the possibility of solving the tuning problem [23]. In [24], an adaptive fuzzy-neural-network controller (FNNC) is developed to a brushless drive system. The FNNC performed a better dynamic performance with shorter settling time and no occurrence of overshoot. The neural network is implemented to minimize the error signal as compared to PI controller. The usage of neural network is critical for improvement of PID controller. In [25], a neural sliding mode controller composed of RBF neural network control and sliding mode control was designed to eliminate the SMC chattering problem. Besides, a neural-network-based feedforward controller was

presented to improve positioning performance in the presence of friction and force ripple that lead to the inaccuracy motion system performance [26]. However, the stability of the overall system cannot be guaranteed and it is complex design due to their unsystematic approaches [27].

Nominal characteristics trajectory following (NCTF) controller consists of three generations, which is NCTF, continuous-motion NCTF (CM-NCTF) and acceleration reference CM-NCTF (AR-CM NCTF). NCTF controller is composed of NCT and a PI compensator. These controllers were proposed on many applications, including one mass rotary system [13], two mass point-to-point (PTP) rotary positioning system [28] and ball screw mechanisms [29, 30]. NCTF controller is a practical controller as it does not require an exact model and parameter identification. NCTF controller is independent of friction characteristic [31]. CM NCTF is an advanced NCTF controller that has been improved the performance of the motion control system in tracking and contouring motions with retaining of PTP motion. CM NCTF is appropriated in all motion control [32]. A CM-NCTF controller with additional of velocity feedforward element was simulated in [29] to clarify its tracking motion performance using an AC driven X-Y ball screw mechanism. Based on the simulation results, it was shown that the proposed controller did improve the tracking performance by reducing the maximum tracking error in high frequency with both small and large working range.

Conventional two-degree-of-freedom (2-DOF) controller consists of a PID compensator and feedforward (FF) element and a feedback compensator for high performance and motion accuracy. PID compensator was designed as a serial compensator, whereas the feedback compensator was designed with pole placement method and the feedforward element was designed based on the simple inverse model of the device [33, 34]. In 1996, the method of designing 2-DOF PID position controller was proposed for linear servo motor drive systems in consideration of the position reference, disturbance, the positioning accuracy and the frequency response on the disturbances and the variation of loads [35]. This controller was using the tuning method, and the control parameters can be gained with the simple calculations. Based on the results, the proposed controller is robustness towards model error and disturbances, besides obtaining the better transient characteristics with no transient vibration, no overshoot and short settling time. Besides, this controller also has been proposed to perform positioning control on an AC servo ball screw driven XY table

[36]. The results had proved the effectiveness of the proposed controller on the tracking performance comparing to the 1-DOF PID controller. A 2-DOF controller with a Disturbance Observer-Based (DOB) was proposed in [37] for disturbance suppression and error reduction. DOB controller, using disturbance estimation techniques, is added for disturbance attenuation and compensation of mechanism uncertainty. A Q-filter, which has been identified as a low pass filter is added to an inverse-model-based DOB to retain the stability by removing the noise and disturbances [21, 38].

Feedforward control is located outside the closed-loop system, and can be designed independently. Therefore, it does not affect the stability of the (feedback) system. In control theory, a feedforward element will increase the control signal. Thus, this control can make a substantial improvement in system, for instant the rapid system response. Feedforward control is an advanced approach that provides enhanced disturbance rejection capability, and it is basically used to reduce the effect of measured disturbances and improve set-point tracking using the process input signal [39]. The exact model and accurate model parameter are required to design a feedforward controller. Feedforward controllers have been used to supplement the feedback controllers under acceptable modelling uncertainties. Additional of feedforward elements brings advantage of transient response [40]. There are two designs of feedforward elements, which are updated control (UC) and updated reference (UR). The feedforward element is added at the input before the plant of the system is called UC, whereas UR means that the added feedforward element is the updated reference. Feedforward filter elements have been proposed for the improvement of tracking performance, but they are sensitive to model errors.

There are several feedforward controls can be found, for example, friction-model-based feedforward approach, $H_2/H\infty$ combined feedforward/feedback controllers, learning feedforward controller, μ-optimal feedforward controllers, adaptive feedforward, feedforward with Zero-Phase-Error-Tracking (ZPETC), feedforward linear quadratic regulator (LQR), Iterative Learning Control (ILC).

A linear model-based feedforward control for improving tracking performance of linear motors was proposed and showed the reduction of the tracking errors due to the limitation of the closed-loop bandwidth from experimental results [41]. In point-to-point (PTP) movement, the settling times of large working range are reduced with the existence of feedforward control [42]. A 2-DOF with feedforward compensator

was designed using coprime factorization approach to improve the transient response of ball screw mechanism. A predictive feedforward PID (PFPID) is an approach that was proposed to achieve fast settling time and limit the overshoot. Acceleration and velocity feedforward are always tuned with a simple gain. This type of feedforward controller usually used to improve the tracking performance of the system.

2.2 CM-NCTF Controller Control Concept

Figure 2.1 shows the structure of CM-NCTF controller. CM-NCTF stands for Continuous-Motion Nominal Characteristics Trajectory Following. The CM-NCTF control consists of two elements, including Nominal Characteristics Trajectory (NCT) and a Proportional-Integral (PI) compensator. NCT serves as a motion reference, which is constructed on a phase plane, based on the open-loop configuration which contains the characteristics of the mechanism. It is constructed using the open-loop deceleration motion of the mechanism. The PI compensator is designed based on the information from NCT, and serve as a motion controller, to ensure the system motion follows the NCT and stop at the origin of NCT. The control law of CM-NCTF controller is same with the conventional NCTF as shown below:

$$U(s) = \left(K_p + \frac{K_I}{s} \right) U_P(s) \tag{2.1}$$

where

$$U_P(s) = sE(s) - E_{NCT}(s) \tag{2.2}$$

$$E(s) = X_r(s) - X(s) \tag{2.3}$$

and

$$E_{NCT}(s) = N(e) \tag{2.4}$$
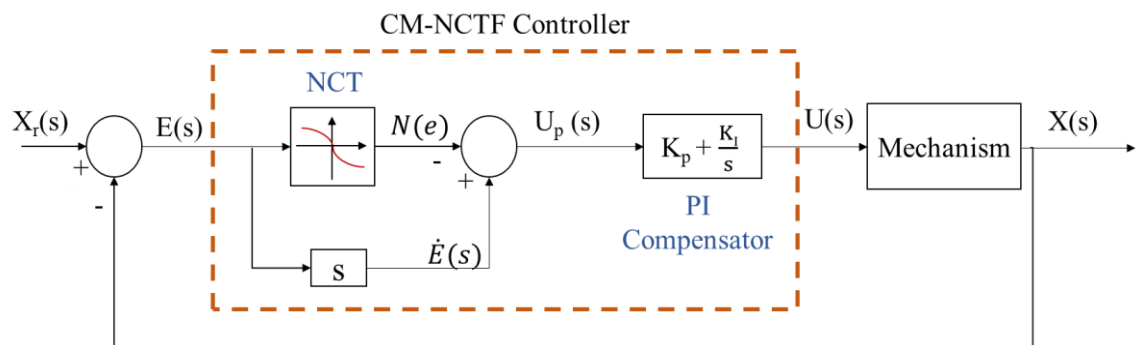
Figure 2.1: Block diagram of CM-NCTF controller structure

Figure 2.2 shows the constructed NCT on phase plane with the displacement and velocity curve. The inclination of the NCT near origin is known as β, refers to the following characteristics of the controller. The mechanism motion is divided into two phases, which is reaching phase and following phase. When the mechanism motion is not at the desired path, signal u_p exists, which is the difference between the location of the mechanism motion and the desired trajectory path $(\dot{x} - \dot{x}_r)$. The PI compensator controls the mechanism motion to reach the trajectory by reducing u_p. When the mechanism motion reaches the desired trajectory path, u_p then become zero. This phase called reaching phase. Following phase means that PI compensator controls the mechanism motion to follow the trajectory of NCT and stops at the origin.

Figure 2.2: Phase on NCT

2.3   Direct Drive System

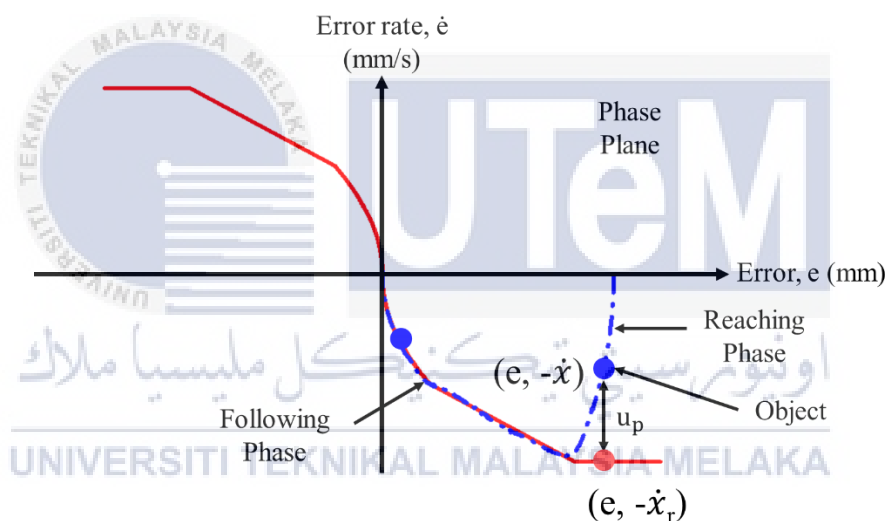Mechanical drives system technology has evolved from the conventional electromechanical feed drive system to direct drive systems to improve the drive performance. There are several types of mechanical drive machine in machine tools, which commonly are rack and pinion system, ball screw drive system and linear direct drive system [43, 38]. Rack and pinion drives (RPD) are linear actuators, virtually unlimited maximum length of the travel and constant dynamic characteristics along the travel [44] as shown in Figure 2.3. Ball screw drive (BSD) system is conventional electromechanical drive system, contained a rotary motor with a transmission element to the slide [45] as shown in Figure 2.4. The transmission element is used to convert the rotary motion into linear motion. This kind of setup has leads to some disadvantages, such as backlash and friction derived from mechanical reduction gear. The pitch tolerances of the element generate transmission errors that may reduce the tracking accuracy. Therefore, the application of conventional electromechanical drive system is limited for a high demand of position, speed and position accuracy [46].
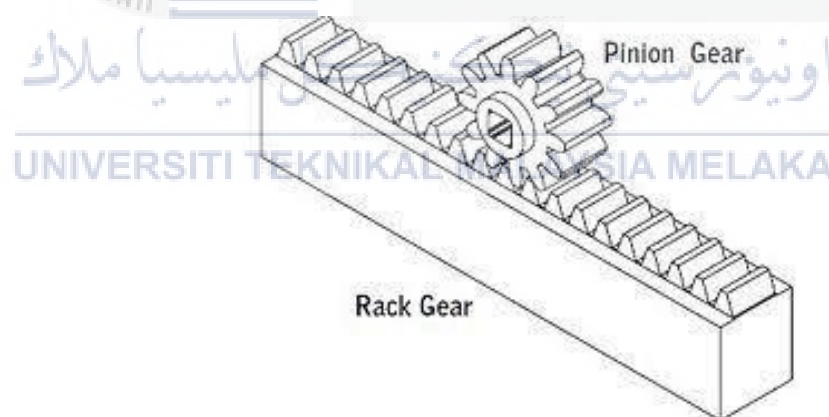
Figure 2.3: Rack and pinion drive system

Figure 2.4: Ball screw drive system

Linear motor is a kind of direct drive system, which is introduced as an enhancement of ball-screw drives system [38] as shown in Figure 2.5. Direct drive systems do not have mechanical transmission device such as screws or gears between motor and the load. By eliminating gear related problems like backlash and friction derived by transmission elements, direct drive system offers high speed and high tracking performance requirements to industry over conventional electromechanical drive system. However, the positioning and tracking accuracy of the system both are also influenced by the disturbance and parameter variations at same time. The first natural frequency normally associated with the ball-screw drive is removed thus extending the bandwidth of the system [38]. This kind of drive system is used when the positioning or tracking performance is required as in high speed machine tools.

Figure 2.5: Linear direct drive (LDD) system

2.4   Structure and Working Principle of Linear Motor

The linear motor has similar working principle as rotary motor. Professor Laithwaited stated the linear motor is an "unwrapped rotary motor", where the rotary motor has rolled out flat as illustrated in Figure 2.6 [47]. Linear motor has its unwrapped and laid out flatted stator, and the moving "rotor" that moves past it in a straight line [48]. Linear direct drive motors are a frameless permanent magnet, three phase brushless servo motor [49]. For brushless linear motor, magnet is in the stationary (primary part) while the coil assembly (armature coil) is in a motion (secondary part) [50].
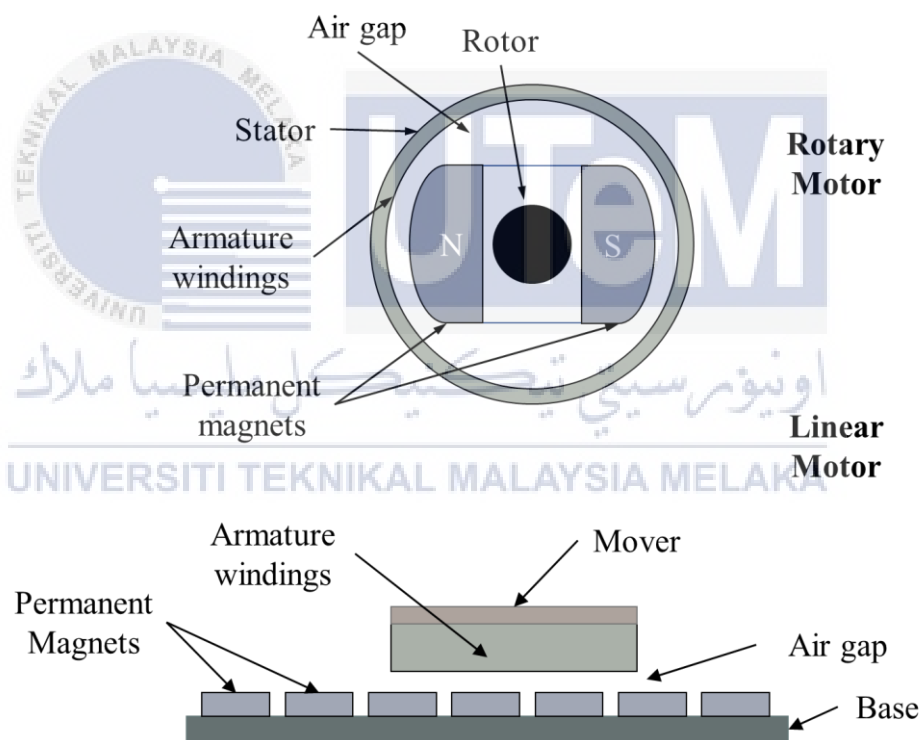

Figure 2.6: Illustration of "unwrapped" rotary motor of linear motor [51]

Based on the right-hand rule of electromagnetic law, a current moving through a coil creates a magnetic field. This field is called electromagnetic field. According to Lorentz's force, a current carrying conductor placed in a magnetic field will experience force. This force generates a linear motion by moving the mover, called thrust force. The thrust force is produced by the interaction between the permanent magnetic field and the electromagnetic field of the three-phase windings. The thrust force is proportional to the magnetic field and the phase currents.

$$\text{Thrust force, } F_{thrust} = K_m I_a \tag{2.5}$$

where

F_{thrust} = thrust force applied to the mover (N)

K_m = motor force constant (N/A)

I_a = current applied to the system (A)

K.K. Tan et al. [6] stated that the nonlinear properties underlying a linear motor system are the friction (Coulomb and viscous) and force ripples (cogging and reluctance forces) arising from inadequacies of the components. Cogging also known as detent or 'no-current' force, that caused by the interaction between the permanent magnet and the iron-cores. Cogging is negligible for iron-less motors [52]. Reluctance force occurs when the current flows, which causes a position dependent forces [53]. Based on [5], the disturbance forces can be assumed as an equivalent force by the unified approach as the parameter of the disturbance forces change irregularly. The friction force is modelled with a kinetic friction model. In the kinetic friction model, the friction force is assumed to be an equivalent friction force, which is dependent of velocity.

$$\text{Friction force, } F_{fri} = bv \tag{2.6}$$

Therefore,

$$F_{fri} = b\dot{x} \qquad (2.7)$$

where

F_{fri} = equivalent friction force generated (N)

v = velocity (m/s)

b = friction coefficient (Ns/m)

x = position of the mover (m)

Based on Newton's Law, a load can only accelerate when there are forces on the load. This force is known as mass variation disturbance. Parameter of mass is a measure of resistance to acceleration. Therefore, the more the mass of the load, the greater the force needed to accelerate the load, thus the greater the acceleration of the motor.
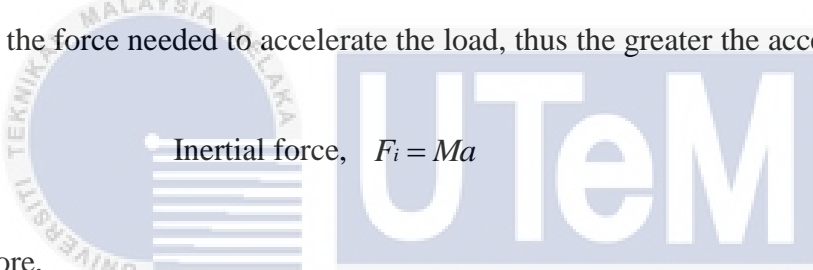
$$\text{Inertial force,} \quad F_i = Ma \qquad (2.8)$$

Therefore,
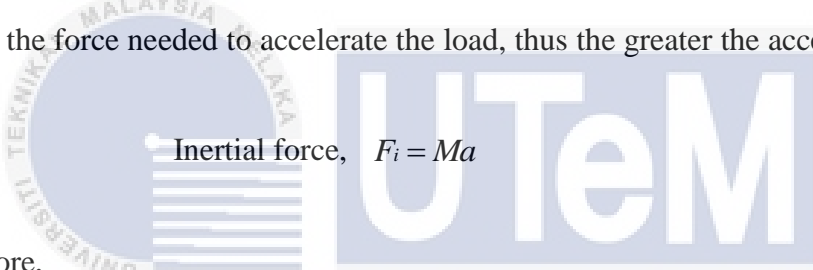
$$F_i = M\ddot{x} \qquad (2.9)$$

where

F_i = inertial force

M = mass of the load (kg)

a = acceleration (m/s²)

The transfer function of the system is determined by using a mass-damper-spring representation as shown in Figure 2.7. The free body diagram of the system is shown in Figure 2.8. The dynamic equation of the motion can be described by

$$M\ddot{x}(t) + b\dot{x}(t) = K_m I_a(t) \tag{2.10}$$

Transfer function of the system in frequency domain can be described by

$$\frac{X(s)}{I_a(s)} = \frac{K_m}{Ms^2 + bs} \tag{2.11}$$
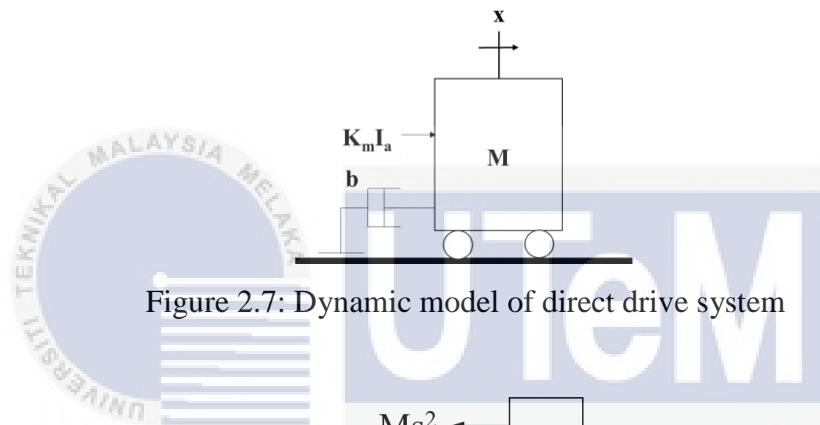
Figure 2.7: Dynamic model of direct drive system
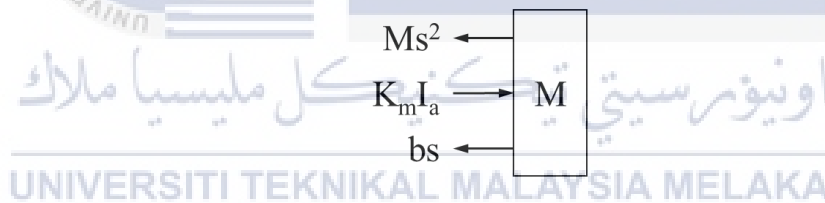
Figure 2.8: Free-body diagram of the direct drive system
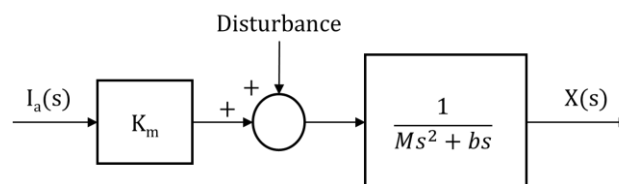
Figure 2.9: Block diagram of direct drive system

CHAPTER 3

METHODOLOGY

3.1   Introduction

This chapter discusses the method used in order to achieve the objectives of the project. The experimental setup is first introduced, then followed by the system modelling. After that, the system design procedure is discussed, which is divided into three parts. In phase 1, the open-loop and closed-loop of uncompensated system are explained with different input signals to evaluate the behaviour of the uncompensated system. The simulation and experimental responses of the open loop system are examined. In phase 2, the CM-NCTF controller is designed. In phase 3, an additional velocity feedforward element is added to the CM-NCTF controller to be compared with the alone CM-NCTF controller.

Table 3.1: Design procedure of the IPMLM system

Phase	Design
1	Uncompensated open-loop and closed-loop constructed
2	CM-NCTF controller designed
3	Additional of feedforward element into controller

3.2   Experimental Setup

The experimental setup of an ironless permanent magnet linear motor (IPMLM) system is illustrated in Figure 3.1. The system consists of following components: a linear motor system, personal computer (PC) with Microbox 2000/2000C and encoder interface. Microbox 2000/2000C is a type of microcontroller, a data acquisition unit to send and receive the signal via Ethernet cable attached to PC. The linear motor system is composed of a U-shaped ironless permanent-magnet linear motor (GLM5001) assembled with two linear guide tracks, and an AC servo driver (GTHD-0062AAF1) which operates in current mode. A linear encoder (RENISHAW RGH24W30D33A) acts as a position feedback which is attached to the mover to measure the displacement of the mover. The specifications of the linear motor are listed in Appendix B. Appendix C shows the pin connection of the direct drive system (IPMLM) to Microbox 2000/2000C.

The motion operation of the system is simple. PC communicates with Microbox (microcontroller) using xPC Target module in Simulink to conduct a real-time simulation. Controller sends the voltage input signal to the ac servo driver based on the command given to produce a linear current of 0.128 A/V to drive the IPMLM mechanism. The controller has a maximum range of ± 10V with sampling frequency of 1 kHz. The IPMLM mechanism is then driven by an AC servo driver (motor driver) in current controlled mode. The displacement of the IPMLM is measured by a linear encoder with resolution of 0.2 µm. Owing to the limitation of the linear encoder, the velocity of the IPMLM can only be achieved at ± 500 mm/s.
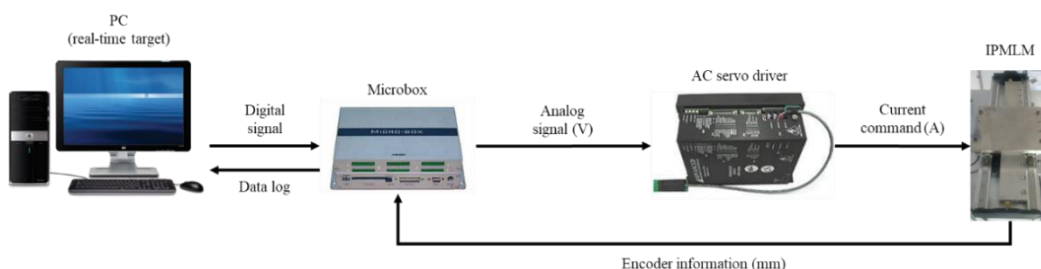
Figure 3.1: Experimental setup of IPMLM system

3.3   System Modelling

The motor considered are brushless permanent magnet linear motor (IPMLM) with epoxy cores. A linear motor consists of a stator and a mover. The motor has a closed magnetic path through the gap since two magnetic plated "sandwich" the coil assembly. The stator induces a multipole magnetic field in the air gap between the magnetic plates. The magnet assembly consists of rare earth magnets, mounted in alternate polarity on the plates. The electromagnetic thrust force is produced by the interaction between the permanent magnetic field in the stator and the magnetic field in the translator driven by the current of the servo amplifier. The linear motors under evaluation are current-controlled three-phase motors driving carriages supported by roller bearing. The mechanism and structure of IPMLM are shown in Figure 3.2 and Figure 3.3 respectively.

Figure 3.32: Ironless Permanent-Magnet Linear Motor (IPMLM) mechanism
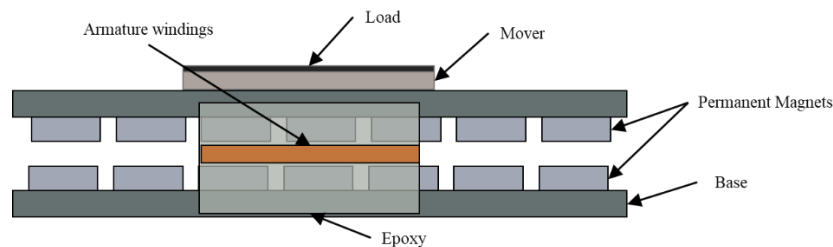
Figure 3.3: Structure of ironless permanent magnet linear motor (IPMLM)

Using mass-damper-spring representation in Figure 3.4, the dynamic equation of the motion of IPMLM can be described as (3.1) and simplified to (3.4);

$$M\ddot{x}(t) + b\dot{x}(t) = K_m K_a u(t) \tag{3.1}$$

K and α are expressed as

$$K = \frac{K_m K_a}{M} \tag{3.2}$$

$$\alpha = \frac{b}{M} \tag{3.3}$$

Rewrite (3.1),

$$\ddot{x}(t) + \alpha\dot{x}(t) = Ku(t) \tag{3.4}$$

where

M = load mass (kg)

b = friction coefficient (Ns/mm)

$K_m K_a$ = force constant of the motor (N/V)

u = voltage input to the motor (V)

The simplified model of IPMLM in frequency domain can be described by (3.5).

$$\frac{X(s)}{U(s)} = \frac{K}{s(s + \alpha)} \tag{3.5}$$
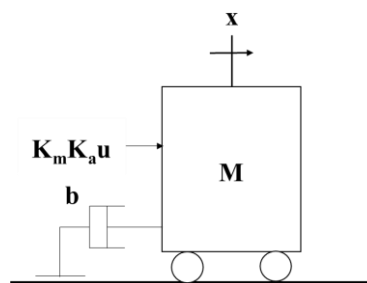
Figure 3.4: Dynamic model of direct drive system IPMLM

3.4   System Design Procedure

Phase I: Open-loop and closed-loop constructed of uncompensated system.

The simulation parameter of IPMLM system is depicted in Table 3.2. The experimental and simulation result response are both observed and depicted in Figure 3.5 [54], using duty cycle of 0.05 s, and amplitude signal of 6 V and 8 V. Figure 3.5 shows that the described model parameters seem to be similar as the real plant parameters. However, the maximum friction may vary from experiments to experiments, thus the value of F_{max} is slightly adjusted. A rectangular input signal is used in open loop, to drive the mechanism (IPMLM) to measure the displacement and velocity. Then, the output signal is observed with different input signals (2 V, 3 V and 5 V) and duty cycles (0.1 s and 0.3 s). In closed loop, a step input signal is used with a unity feedback for correction purpose. The transient behaviour is observed with 0.1 s of duty cycle and different input signals (1 mm, 3 mm, 5 mm, 7 mm, 9 mm and 10 mm).

Table 3.2: Model parameters of IPMLM

Symbol	Description, unit	Value
M	Load mass, kg	3
K_m	Force constant, N/A	33
K_a	Voltage-to-current gain, A/V	0.128
b	friction coefficient, Ns/mm	10
F_{max}	Maximum friction, N	4.35
T_s	Sampling time, ms	1
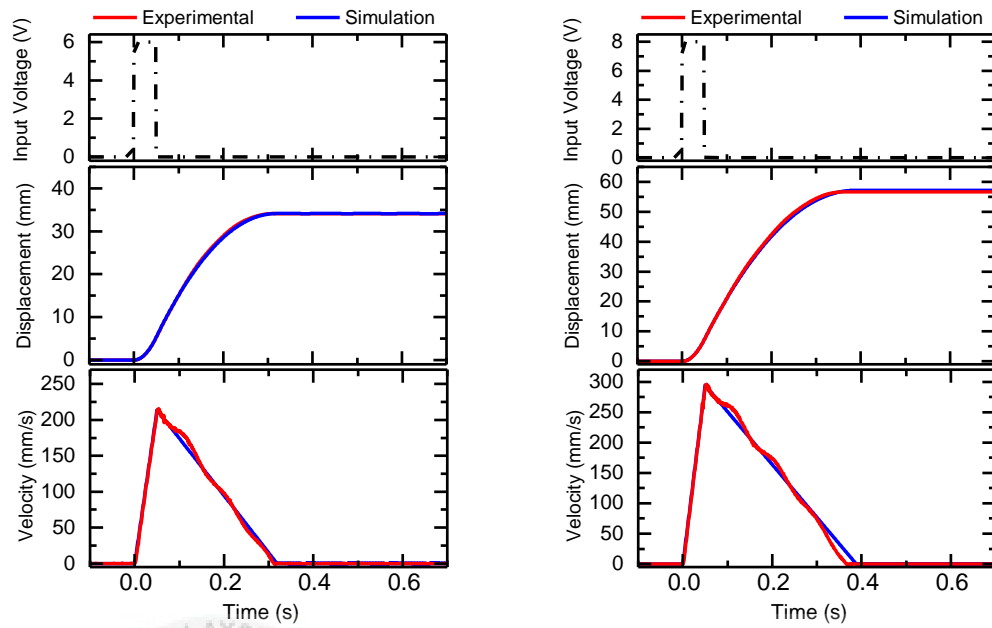
(a) Impulse signal: amplitude 6 V, duty cycle 0.05 s

(b) Impulse signal: amplitude 8 V, duty cycle 0.05 s

Figure 3.5: Open loop responses of IPMLM

Phase II: CM-NCTF controller designed.

The structure of CM-NCTF controller is presented in Figure 3.6, and its design procedures is discussed as in [14]. The design procedures of CM-NCTF controller is similar with a conventional NCTF controller as discussed in [9, 30, 55], comprised of three major steps as following:

a. Drive the mechanism with a suitable input in open-loop configuration.

A suitable rectangular input signal is used to drive IPMLM in open loop and the corresponding displacement and velocity are measured, the input signal is 2 V with 0.1 s of duty cycle, as shown in Figure 3.7. The parameters of the open loop configuration are presented in Table 3.3.

b. Construct the NCT on phase plane with obtained open-loop response.

NCT is constructed on a phase plane using the displacement and velocity obtained from open-loop response during deceleration, as shown in Figure 3.9. The inclination of NCT near origin (slope) is referred as β equals to 558 s^{-1}, is taken to be used in this experiment. A low pass filter is added to reduce the noise from the derivation action for high frequency.

c. Design PI compensator based on open-loop responses and NCT information.

A practical stability analysis is determined to select a suitable parameter of PI compensator. The values of K_p and K_i of the PI compensator are 0.24 Vs/mm and 2.69 V/mm respectively based on the stability analysis shown in Figure 3.10. A conditional freeze anti windup is added to reduce the overshoot caused by the integrator [9]. The structure of CM-NCTF with anti-windup element control is depicted in Figure 3.11.
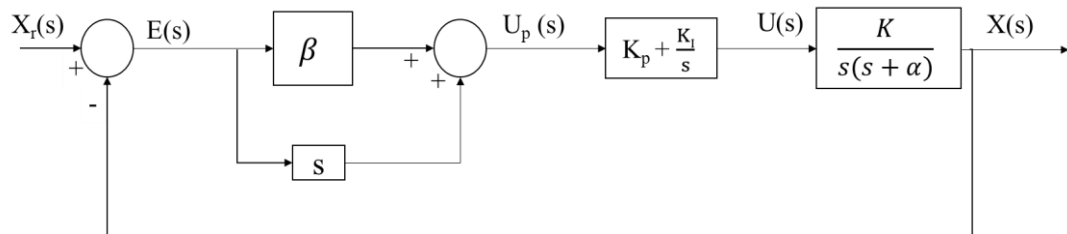
Figure 3.6: Block diagram of CM-NCTF controller
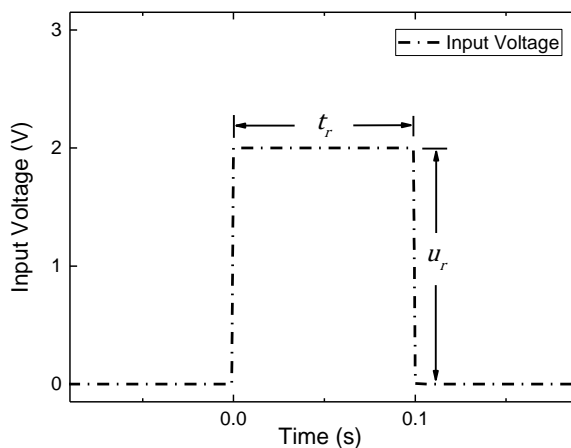
Figure 3.7: Input signal to drive IPMLM
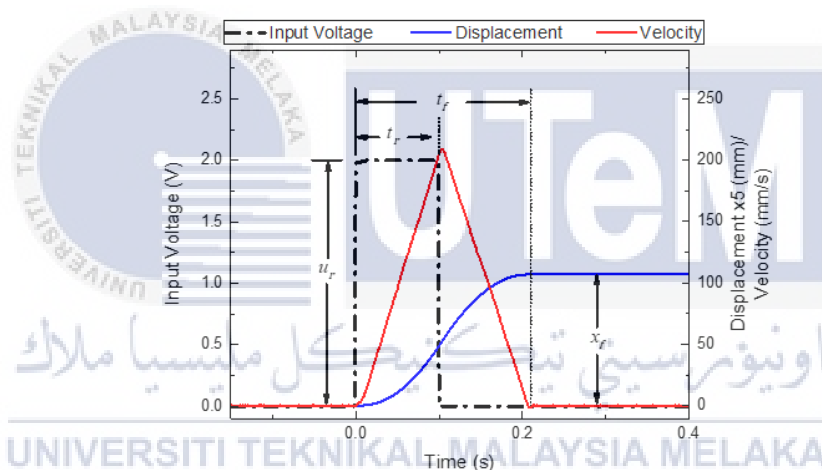
Figure 3.8: Open loop response of 2 V input signal with 0.1 s of duty cycle

Table 3.3: Parameters of the IPMLM open loop response

Parameters	Description, Unit	Value
u_r	Amplitude of input signal, V	2
t_r	Time width of the input signal, s	0.1
t_f	Total time of motion, s	0.2
x_f	Final displacement, mm	21.4
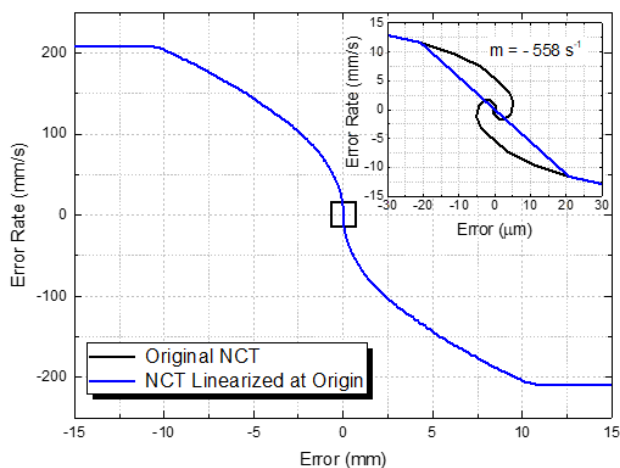
Figure 3.9: Constructed NCT [14]
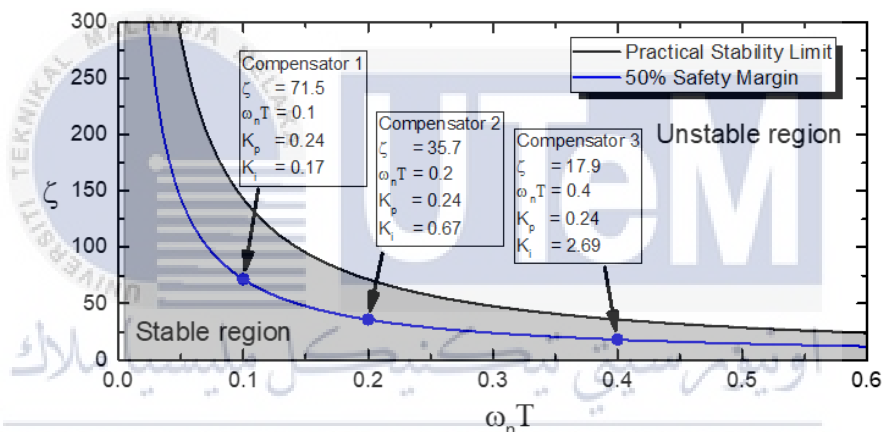
Figure 3.10: Different PI compensators on 50 % safety margin of practical stability

limit [14]
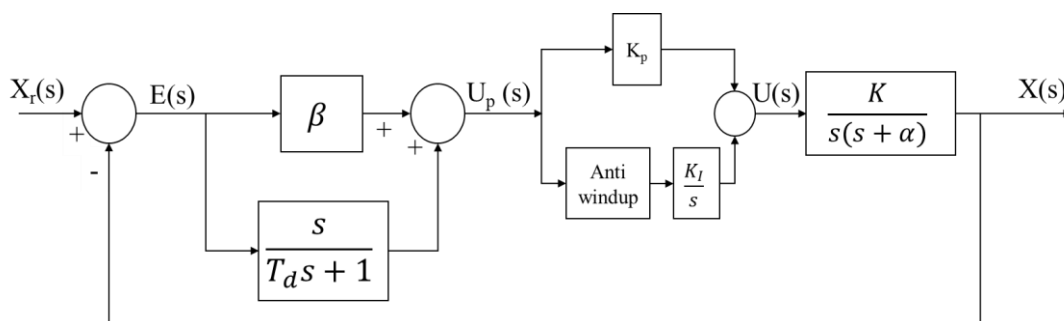
Figure 3.11: CM-NCTF controller with anti-windup element

In Figure 3.9, the relationship between error rate, $\dot{e}$ and error, e can be written as

$$\frac{\Delta\dot{e}}{\Delta e} = -m = \beta \tag{3.6}$$

Comparing the overall transfer function of compensated system with a general second order equation is given as ($\alpha = \beta$ when derivative of reference equals zero);

$$\frac{X(s)}{X_r(s)} = \frac{K_p K s + K_i K}{s^2 + K_p K s + K_i K} = \frac{2\zeta\omega_n s + \omega_n^2}{s^2 + 2\zeta\omega_n s + w_n^2} \tag{3.7}$$

The gain compensator of K_p and K_i are given as

$$K_p = \frac{2\zeta\omega_n}{K} \tag{3.8}$$

$$K_i = \frac{\omega_n^2}{K} \tag{3.9}$$

Phase III: Additional of feedforward element on CM-NCTF controller.

The velocity feedforward method is used and evaluated in this experiment. The positioning performance of the compensated system is evaluated in point-to-point (PTP) and tracking motion, to show the effectiveness of the add-on feedforward elements on the system. The experiment is conducted by using the large working range of step input of 30 mm and 50 mm, and high frequency of sinusoidal input of 5 Hz. This section is to introduce an alternative approach, see whether it is suitable to address the control design problem.

The structure of the CM-NCTF with velocity feedforward controller is presented in Figure 3.12. This structure shows that the feedforward signal, $\dot{x}_r$ can help the mechanism to move faster. Based on [29], the largest feedforward gain, K_{ff} to be used in the experiment is based on β, which is 0.0035 Vs/mm, referring to $\frac{2}{\beta}$. There are another two gains of 0.00015 and 0.00020 Vs/mm are to be used in tracking motion with only 1 mm input signal.
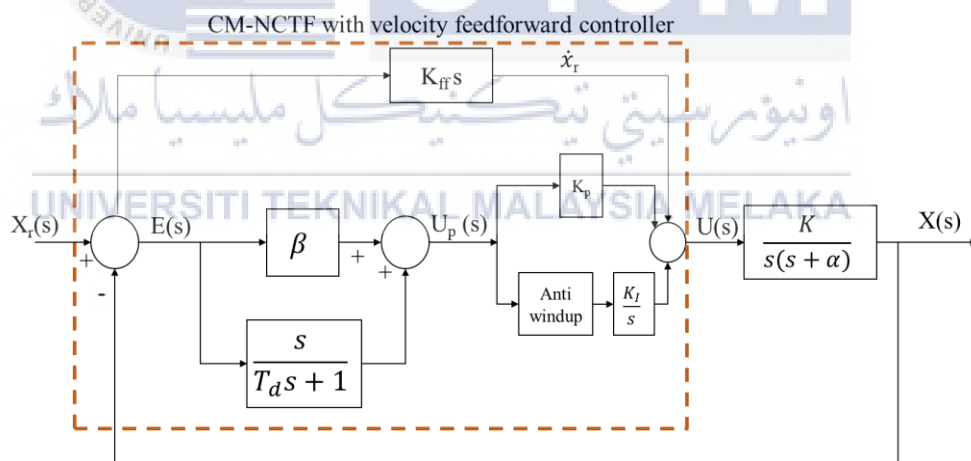
Figure 3.12: Structure of CM-NCTF controller with a velocity feedforward

CHAPTER 4

RESULTS AND DISCUSSION

4.1 Uncompensated System Response Analysis

In an open-loop system, the output signal cannot be measured as there is no feedback for comparison with the input signal. So, the system just follows its input command signal regardless of the final result. When the duty cycle of the system is set from 0.1 s to 0.3 s with the same amplitude of 3 V, the system decelerates non-smoothly as shown in Figure 4.2 (b). It is due to the limitation of the device, besides with the large displacement and high velocity. In this experiment, the achievable velocity of the IPMLM is only ± 500 mm/s. Therefore, each input signal should be taken under consideration to fix an operating position in an open loop system, so the system moves smoothly. In closed-loop system, at step input signal of 1 mm, the overshoot percentage of the system is small with only 0.13%. However, the rise time is 0.06 s, very slow response. At step input signal of 5 mm, the overshoot percentage of the system is quite high which has increased to 75.52%. However, the rise time is 0.04 s, fast response. Thus, it can be concluded that, as the step input signal increase (becomes large), the overshoot percentage and the settling time also increase, but the rise time decreased.

It is important to implement controller to regulate the behaviour of the system to achieve a fast rise time, minimum overshoot with small steady-state error. The implemented controller should reduce the overshoot percentage and steady-state error, and reduce the rise time simultaneously to enhance the system performance. The controller to be designed is CM-NCTF controller with velocity feedforward element, and the its positioning performance will be evaluated in terms of point-to-point (PTP) and tracking motion.
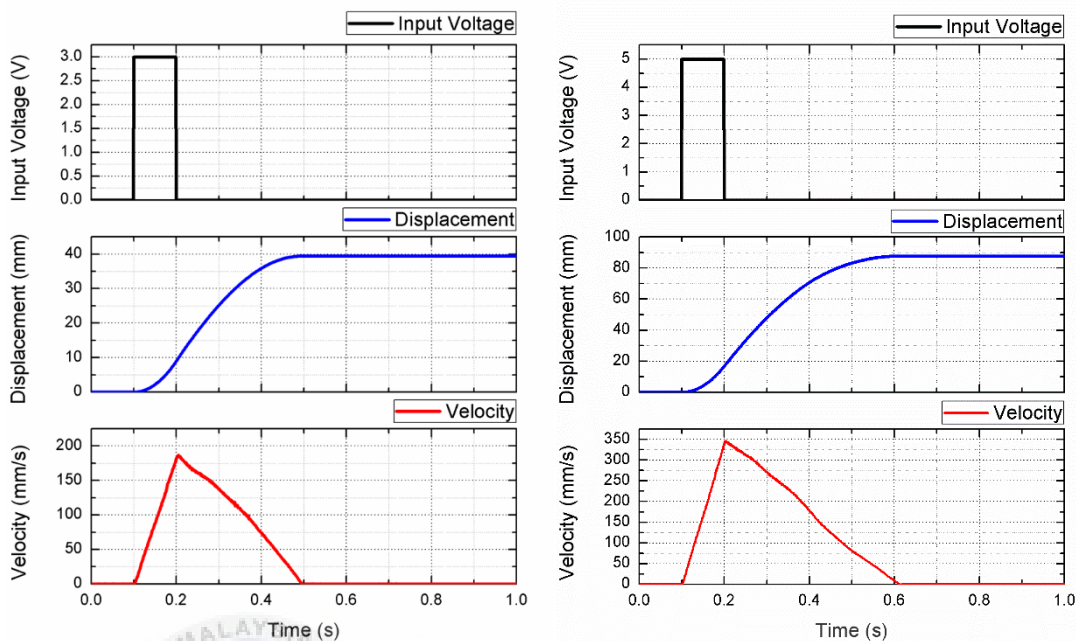
(a) 3 V input signal   (b) 5 V input signal

Figure 4.1: Uncompensated open-loop response with 0.1 s of duty cycle
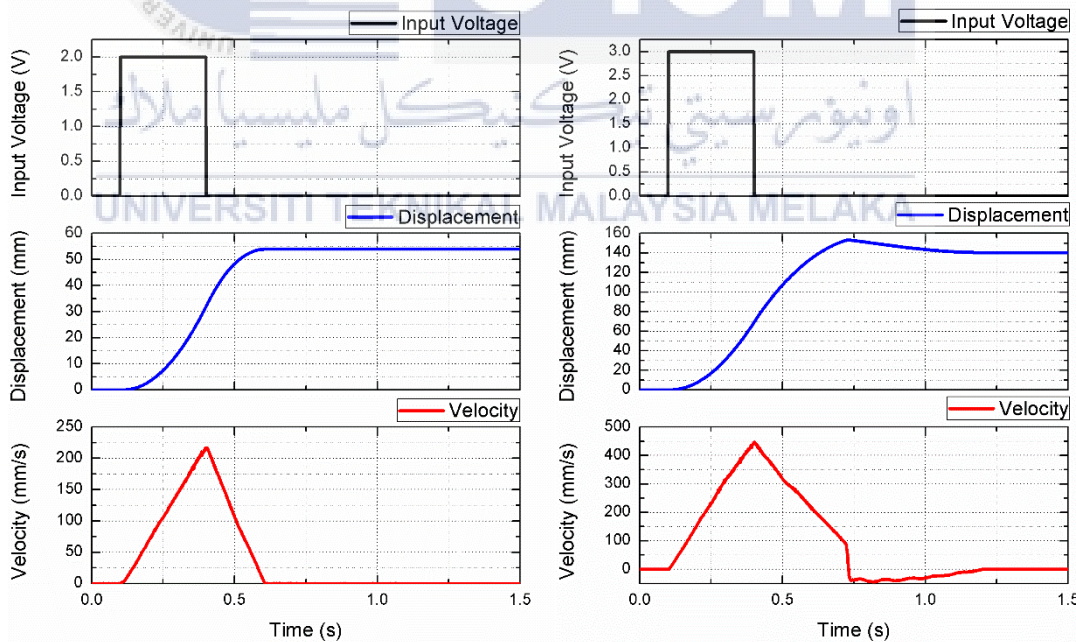
(a) 2 V input signal   (b) 3 V input signal

Figure 4.2: Uncompensated open-loop response with 0.3 s of duty cycle
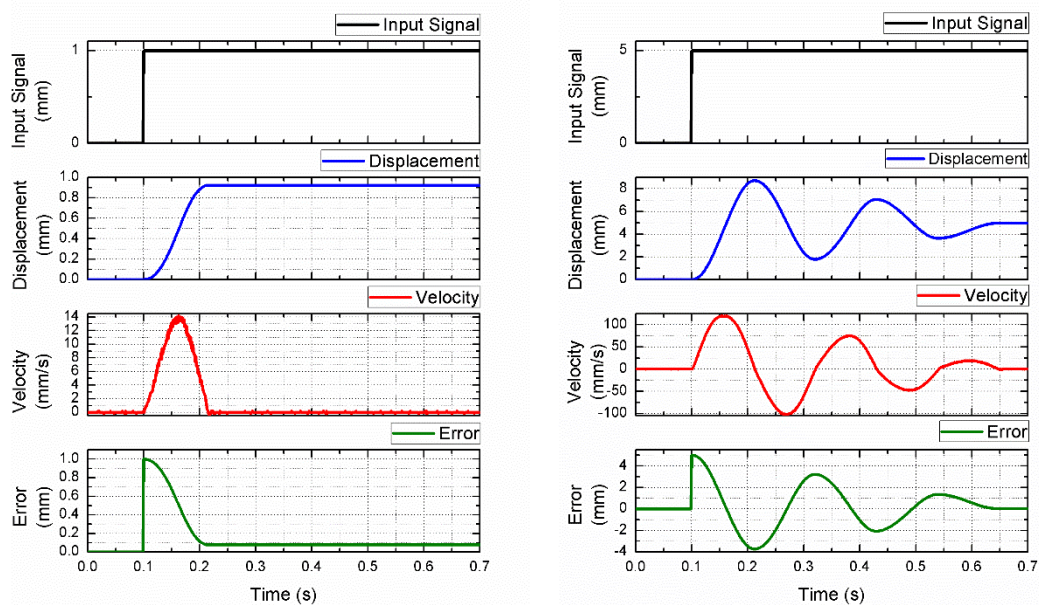
(a) 1 mm input signal   (b) 5 mm input signal

Figure 4.3: Uncompensated closed-loop behaviour with different input signals

Table 4.1: Uncompensated closed-loop behaviour with 0.1 s of duty cycle in different input signals

Input Signal (mm)	Rise Time (s)	Settling Time (s)	Overshoot Percentage (%)	Steady-state Error
1	0.06	0.20	0.13	0.08
3	0.04	0.31	58.75	0.09
5	0.04	0.63	75.52	0.03
7	0.04	0.64	73.43	0.19
9	0.04	0.84	84.14	0.17
10	0.04	1.27	97.20	0.44

4.2   Analysis of Positioning Performance of Compensated System

The additional of velocity feedforward method is evaluated in this experiment by comparing with the alone CM-NCTF controller. The positioning performance of the compensated system are evaluated in point-to-point (PTP) and tracking motion, to show the effectiveness of the add-on feedforward elements on the system. The large working range of the step inputs of 30 mm and 50 mm are to be used to be examined in PTP motion, whereas the high frequency of sinusoidal input of 5 Hz with amplitude of 1 mm and 5 mm are to be used in tracking motion.

The CM-NCTF controller with and without velocity feedforward is simulated to IPMLM. The positioning performance of CM-NCTF with and without velocity feedforward gain are examined through experimental. The transient response of the system compensated using CM-NCTF controller with additional velocity feedforward element are presented in Table 4.2. The transient response included are rise time, settling time, percentage overshoot and steady-state error. The tracking response of the system is presented in Table 4.3 and 4.4, using same frequency of 5 Hz with different velocity gain. The evaluation is taken through comparison between CM-NCTF with and without velocity feedforward element.

Table 4.2: Transient analysis of CM-NCTF controller without and with velocity feedforward $K_{ff} = 0.0035$ *Vs/mm* in different input signals

Input Signal (mm)	Controller	Rise Time (s)	Settling Time (s)	Overshoot Percentage (%)	Steady-state Error
30	CM-NCTF	0.46	0.62	0	0
	CM-NCTF with velocity feedforward	0.46	0.62	0	0
50	CM-NCTF	0.71	0.94	0	0
	CM-NCTF with velocity feedforward	0.71	0.94	0	0
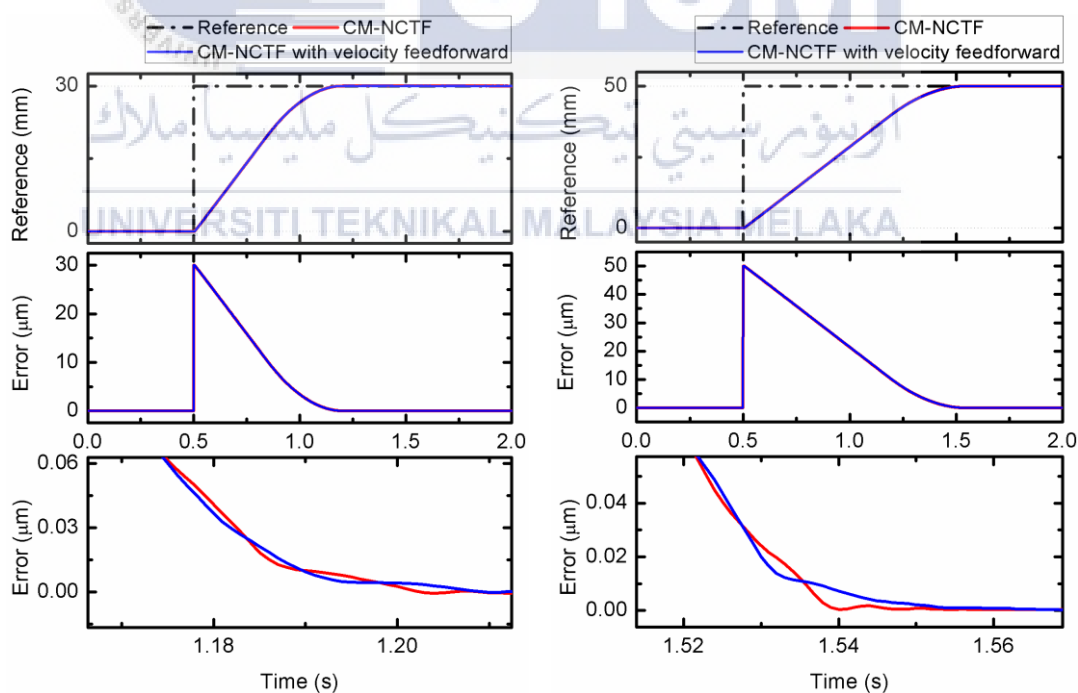
(a) Step input of 30 mm   (b) Step input of 50 mm

Figure 4.4: Transient response of CM-NCTF with and without velocity feedforward $K_{ff} = 0.0035$ *Vs/mm*

Table 4.3: Maximum tracking error of CM-NCTF controller without and with

velocity feedforward $K_{ff} = 0.0035$ *Vs/mm* in amplitude variation for 5 Hz frequency

Frequency (Hz)	Amplitude (mm)	Maximum Error, E_{max} (µm)	
		CM-NCTF	CM-NCTF with velocity feedforward
5.0	1	15.4	15.1
	5	79.0	116.0
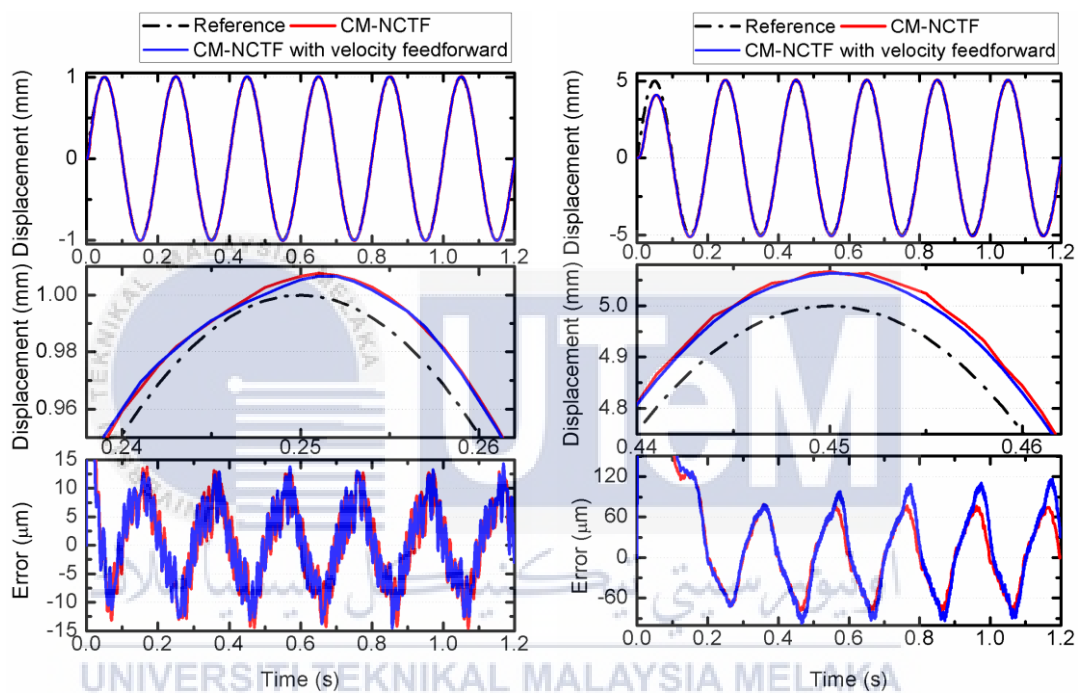
(a) Reference sinusoidal of 1 mm   (b) Reference sinusoidal of 5 mm

Figure 4.5: Experimental tracking response of CM-NCTF with and without

velocity feedforward element $K_{ff} = 0.0035$ *Vs/mm* for 5 Hz

Table 4.4: Maximum tracking error of CM-NCTF controller without and with velocity feedforward in 5.0 Hz and 1 mm with different feedforward gain, K_{ff}

Frequency (Hz)	Amplitude (mm)	K_{ff} (Vs/mm)	Maximum Error, E_{max} (μm)
5.0	1	0.00015	14.6
		0.00020	13.9

(a) $K_{ff} = 0.00015$ *Vs/mm*   (b) $K_{ff} = 0.00020$ *Vs/mm*
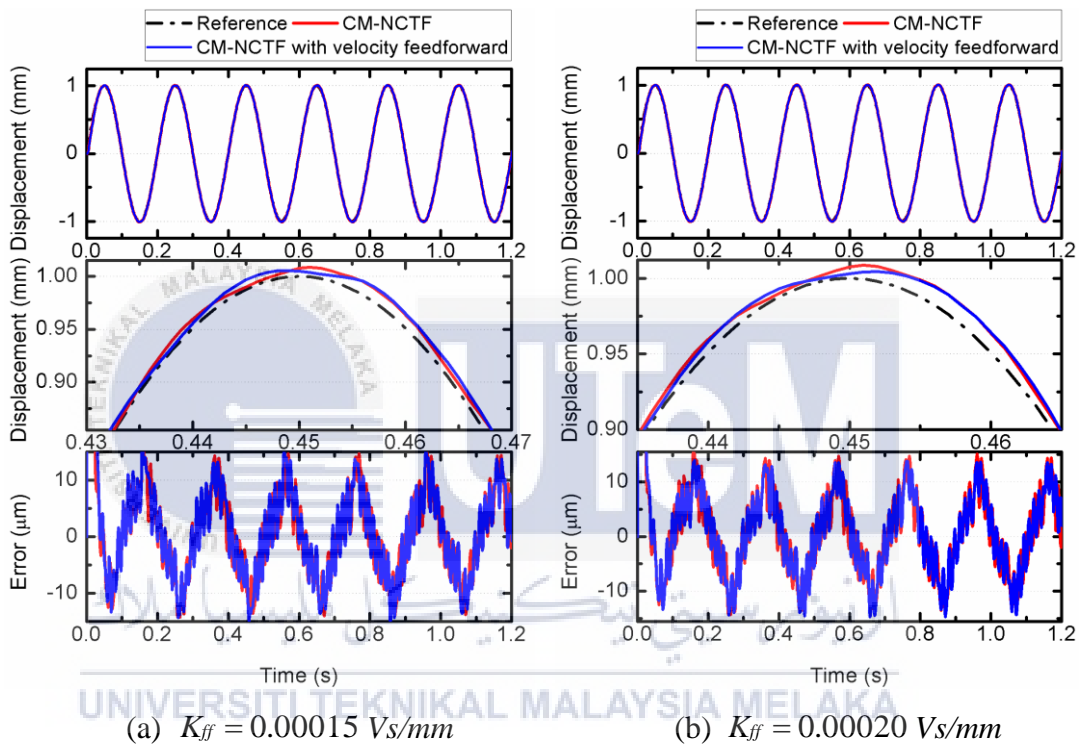
Figure 4.6: Experimental tracking response of CM-NCTF with and without velocity feedforward element for 5 Hz and amplitude of 1 mm with different feedforward gain

When the step inputs of 30 mm and 50 mm are applied to the system, the proposed controller does not show any different or improvement compared to the CM-NCTF controller as shown in Table 4.2 and Figure 4.4. The system does not contain any overshoot and steady-state error. However, the transient response of the system remains the same, very slow motion. Therefore, it can be concluded that the additional velocity feedforward element does not show any effective on the system in point-to-point motion.

In tracking performance, the frequency of the sinusoidal input used is 5 Hz, with sampling time of 1 millisecond. The amplitude of the sinusoidal input is firstly set to 1 mm and 5 mm. The maximum velocity feedforward gains used is 0.0035 Vs/mm. The maximum peak error of the CM-NCTF controller and CM-NCTF with velocity feedforward controller at 1 mm are 15.4 micrometre and 15.1 micrometre respectively. It seems that the velocity feedforward has perform slightly tracking improvement on the system as shown in Figure 4.5. However, Table 4.3 shows that, at the high reference input of 5 mm, the maximum tracking error has increased nearly 45 % by adding the velocity feedforward element inside the system. When the system moves at very high motion of 5 Hz at high input signal of 5 mm, the friction occurs and cause the system noisy, leading to non-smooth and inaccuracy of the positioning performance. Therefore, the large working range of 5 mm at high frequency is not suitable to be used, due to noise and restrictions of the system (encoder resolution is 0.2 µm and working range of the motor is only ± 100 mm). Next, the experiment is conducted using only one small sinusoidal input signal of 1 mm.

Then, using the tuning method, the feedforward gain is changed to 0.00015 Vs/mm. The CM-NCTF with velocity feedforward controller has a maximum tracking error of 14.6 µm as shown in Table 4.4. The tracking error is decreased only 0.8 difference compared to CM-NCTF controller with large error of 15.4 µm. The gain is once again tuned to a slightly high to 0.00020 Vs/mm. The maximum tracking error of the proposed controller (CM-NCTF with velocity feedforward) decrease around 10 % as compared to the only CM-NCTF controller. Figure 4.6 shows the experimental tracking response of the proposed controller with different gain at 5 Hz, compared to the CM-NCTF controller. Since the CM NCTF with velocity feedforward controller has achieve slightly reduction on the tracking error as the sinusoidal input signal supplied, it shows that the CM NCTF with velocity feedforward controller has contribute a slightly faster response compared to the CM NCTF controller as expectation in tracking motion, but not in point-to-point motion.

CHAPTER 5

CONCLUSION AND RECOMMENDATIONS

5.1   Conclusion

From [14], the CM-NCTF controller has achieve a good performance in point-to-point motion with zero steady-state error and overshoot occurrence. However, the CM-NCTF controller shows the slower speed response with long rise time and settling time. Besides, with existence of CM-NCTF controller only, the motion performance showed the low tracking performance at high frequency motion [29]. Thus, an additional of feedforward element on the system is proposed to improve the positioning performance.

In this project, a CM-NCTF with velocity feedforward element controller is implemented to ironless permanent-magnet linear motor (IPMLM), and the positioning performance are then evaluated and examined in point-to-point and tracking motion. However, the experimental results show that the CM NCTF with velocity feedforward gain could not improve the transient response in point-to-point performance and it has less influence in tracking performance as the amplitude of the sinusoidal is varied at high frequency. As the frequency of the reference signal increased, the velocity of the system will increase, and same to relative viscous friction, thus the dynamic model of the plant will be changed. As a conclusion, the CM-NCTF controller with velocity feedforward element managed to compensate the small variation and has the smallest tracking motion error, but it is impractical at high amplitude signal with high velocity. In large working range (displacement), the actuator saturation problem may happen since the working range of the linear motor is only ± 100 mm, that may lead to the deterioration of the positioning performance of the linear motor.

5.2   Recommendation

From the experiment, the additional velocity feedforward element shows a small improvement on the tracking performance but it does not show a great impact in PTP and tracking motion on the system. Thus, it is advised to use a suitable controller to highly improve the positioning performance of this kind of the system (direct drive system). In future, it is suggested to implement an optimal feedforward method to improve the tracking performance, especially in high frequency. A more systematic design methods for the feedforward is important to be used to achieve the performance. However, the optimal feedforward method requires a deep understanding on control knowledge and consist of model-based design, that may consume longer time to obtain the accurate and exact model parameters. The performance accuracy depends on the accuracy model identification.

REFERENCES

[1] A. Slocum, "Fundamentals of Design," *Constructist Foundations,* vol. 10, no. 1, pp. 0-23, 2008.

[2] B. Yao and L. Xu, "Adaptive robust motion control of linear motors for precision manufacturing," *Mechatronics,* vol. 12, no. 4, pp. 595-616, 2002.

[3] L. Bascetta, P. Rocco and G. Magnani, "Force ripple compensation in linear motors based on closed-loop position-dependent identification," *IEEE/ASME Transactions on Mechatronics,* vol. 15, no. 3, pp. 349-359, 2010.

[4] C. Röhrig, "Force Ripple Compensation of Linear Synchronous Motors," *Asian Journal of Control,* vol. 7, no. 1, pp. 1-11, March 2005.

[5] S. Komada, M. Ishida and T. H. e. al., "Disturbance observer-based motion control of direct drive motors," *IEEE Transactions on Energy Conversion,* vol. 6, no. 3, pp. 553-559, 1991.

[6] K. K. Tan, S. N. Huang and T. H. Lee, "Robust adaptive numerical compensation for friction and force ripple in permanent-magnet linear motors," *IEEE Transactions on Magnetics,* vol. 38, no. 1, pp. 221-228, 2002.

[7] "Dictionary Of Engineering," [Online]. Available: http://www.dictionaryofengineering.com/definition/position-control-system.html. [Accessed 03 October 2017].

[8] F. Yakub and R. Akmeliawati, "Study review on nominal characteristic trajectory following controller for point-to-point positioning systems," in *2012 7th IEEE Conference on Industrial Electronics and Applications (ICIEA)*, 2012.

[9] S. H. Chong and K. Sato, "Practical control of non-friction mechanism for precision positioning," in *2008 International Conference on Control, Automation and Systems*, Seoul, South Korea, 2008.

[10] S. H. Chong and K. Sato, "Practical and robust control for precision positioning systems," in *2011 IEEE International Conference on Mechatronics*, Istanbul, Turkey, 2011.

[11] Y. J. Zhao, Q. L. Wang, J. X. Xu and C. Y. Wang, "A fuzzy sliding mode control based on model reference adaptive control for permanent magnet synchronous linear motor," in *2007 2nd IEEE Conference on Industrial Electronics and Applications*, Harbin, China, 2007.

[12] S. Rajan and S. Sahadev, "Performance Improvement of Fuzzy Logic Controller Using Neural Network," *Procedia Technology,* vol. 24, pp. 704-714, 2016.

[13] J. E. Foo, S. H. Chong, R. M. Nor and S. L. Loh, "Positioning Control of a One Mass Rotary System with CM-NCTF Controller," *Journal of Telecommunication, Electronic and Computer Engineering,* vol. 8, no. 11, pp. 125-129, 2016.

[14] J. E. Foo and e. al., "Positioning Control of an Ironless Linear Motor with Continuous Motion Nominal Characteristic Trajectory Following Controller," 2017.

[15] N. S. Nise, Control Systems Engineering, John Wiley & Sons, Inc., 2008.

[16] C. Shin-Horng and S. Kaiji , "Practical and robust control for precision positioning systems," in *2011 IEEE International Conference on Mechatronics*, Istanbul, Turkey, 2011.

[17] S. Vaishnav and Z. Khan, "Design and performance of PID and fuzzy logic controller with smaller rule set for higher order system," in *Proceedings of the World Congress on Engineering and Computer Science*, San Francisco, USA, 2007.

[18] V. Utkin, "Sliding Mode Control," in *Control System, Robotics and Automation: Nonlinear, Distributed, and Time Delay Systems-II*, vol. 13, H. D. Unbehauen, Ed., Columbus,Ohio, USA, EOLSS Publications.

[19] *Sliding Mode Control.*

[20] N. Hasim, S. H. Chong and H. K. Khor, "Disturbance Observer-Based Motion Control for a Simple Direct Drive System," *Journal of Telecommunication, Electronic and Computer Engineering,* vol. 8, no. 5, pp. 41-47, 2016.

[21] C. Kempf and S. Kobayashi, "Disturbance observer and feedforward design for a high-speed direct-drive positioning table," *IEEE Transactions on Control Systems Technology,* vol. 7, no. 5, pp. 513-526, 1999.

[22] S. Chong and K. Sato, "Practical and robust control for precision motion: AR-CM NCTF control of a linear motion mechanism with friction characteristics," *IET Control Theory & Applications,* vol. 9, no. 5, pp. 745 - 754, 2015.

[23] D. van Cleave and K. Rattan, "Tuning of Fuzzy Logic Controler using Neural Network," in *Proceedings of the IEEE 2000 National Aerospace and Electronics Conference. NAECON 2000. Engineering Tomorrow (Cat. No.00CH37093)*, Dayton, OH, USA, USA, 2000.

[24] A. Rubaai, D. Ricketts and M. Kankam, "Development and implementation of an adaptive fuzzy-neural-network controller for brushless drives," *IEEE Transactions on Industry Applications,* vol. 38, no. 2, pp. 441-447, 2002.

[25] L. Long, G. Zhongping and T. Jingfeng, "Neural network-sliding mode control of permanent magnet synchronous linear motor," in *2016 Chinese Control and Decision Conference (CCDC)*, Yinchuan, China, 2016.

[26] G. Otten, T. J. A. D. Vries, J. V. Amerongen, A. M. Rankers, E. W. Gaal and A. Working, "Linear Motor Motion Control Using a Learning Feedforward Controller," in *IEEE/ASME Transactions on Mechatronics*, 1997.

[27] F. Yakub and R. Akmeliawati, "Study review on nominal characteristic trajectory following controller for point-to-point positioning systems," in *2012 7th IEEE Conference on Industrial Electronics and Applications (ICIEA)*, Singapore, 2012.

[28] M. F. M. Yakub, W. Martono and R. Akmeliawati, "Performance evaluation of improved practical control method for two-mass PTP positioning systems," in *2010 IEEE Symposium on Industrial Electronics and Applications (ISIEA)*, Penang, Malaysia, 2010.

[29] N. Hasim and e. al., "CM NCTF with Velocity Feedforward Controller Design for Tracking Control of an AC Driven X-Y Ball Screw Mechanism," in *17th Asia Simulation Conference, AsiaSim 2017*, 2017.

[30] W. K. Hee, S. H. Chong and A. Amran, "Selection of PI compensator parameters for NCTF controller based on practical stability limit," in *2014 IEEE*

International Conference on Control System, Computing and Engineering (ICCSCE 2014), Batu Ferringhi, Malaysia, 2014.

[31] S.-H. Chong and K. Sato, "Practical controller design for precision positioning, independent of friction characteristic," *Precision Engineering,* vol. 34, no. 2, pp. 286-300, 2010.

[32] K. Sato and G. J. Maeda, "A practical control method for precision motion—Improvement of NCTF control method for continuous motion control," *Precision Engineering,* vol. 33, no. 2, pp. 175-186, 2009.

[33] Hama, T. and Sato, K., "High-speed and high-precision tracking control of ultrahigh-acceleration moving-permanent-magnet linear synchronous motor," *Precision Engineering,* vol. 40, pp. 151-159, 2015.

[34] Lee, C. and Salapaka, S. M., "Two degree of freedom control for nanopositioning systems: Fundamental limitations, control design, and related trade-offs," in *Proceedings of the American Control Conference*, Hyatt Regency Riverfront, St. Louis, MO, USA, 2009.

[35] Yamamoto, S., Ara, T., Sugiura, M., Sawaki, J. and Matsuse, K., "The Basic Characteristics of Two-Degree-of-Freedom PID Position Controller using Simple Design Method for Linear Servo Motor Drives," in *Advanced Motion Control, 1996. AMC '96-MIE. Proceedings., 1996 4th International Workshop on*, Mie, Japan, 1996.

[36] Ong, Y.T., Chong, S.H. and Hee, W.K., "Positioning Control of XY Table Using 2-DOF PID Controller," *Applied Mechanics and Materials,* vol. 761, no. May 2015, pp. 137-141, 2015.

[37] Wang, Y., Nam, K., Fujimoto, H. and Hori, Y., "Robust roll and yaw integrated control using 4 wheel steering based on yaw moment and lateral force observers," in *Proceedings of the IEE of Japan Technical Meeting Record*, Japan, 2011.

[38] J. Zamberi , Disturbance Compensation for Machine Tools with Linear Motor Drives, Belgium, 2008.

[39] Faanes, A. and Skogestad, S., "Feedforward Control under the Presence of Uncertainty," *European Journal of Control,* vol. 10, no. 1, pp. 30-46, 2004.

[40] Chen, Xu and Tomizuka, Masayoshi, "Transient Enhancement in Add-on Feedforward Algorithms for High-performance Mechatronic Systems," *IFAC Proceedings Volumes,* vol. 47, no. 3, pp. 7214-7220, 2014.

[41] Y.J. Li and S.C. Tien, "Linear Model-Based Feedforward Control For Improving Tracking Performance of Linear Motor," *Asian Journal of Control,* vol. 16, no. 6, pp. 1602-1611, 2014.

[42] R.J.E. Merry, Performance-driven control of nano-motion systems, Netherlands: Technische Universiteit Eindhoven, 2009.

[43] N. HIDAYAH, "Design Of PID And Nonlinear PID Controller For Tracking Performance Of XY Table Ball Screw Drive System," 2015.

[44] C. Ehrmann, P. Isabey and J. Fleischer, "Condition monitoring of rack and pinion drive systems: necessity and challenges in production environments," *Procedia CIRP,* vol. 40, pp. 197-201, 2016.

[45] Q. Xie, "Modeling and Control of Linear Motor Feed Drives for Grinding Machines," p. 124, 2008.

[46] P. G., "A Comparison of Linear and Conventional Electromechanical Dives," *CIRP Annals,* vol. 47, no. 2, pp. 541-548, 1998.

[47] AEROTECH, Linear motors Application Guide, Science of Motion, 2002.

[48] W. C., "Explain that Stuff," 9 May 2017. [Online]. Available: http://www.explainthatstuff.com/linearmotor.html. [Accessed 1 October 2017].

[49] K. Corporation., "Kollmorgen Direct Drive Linear Motor Selection Guide". UK 2017.

[50] Y. Altintas, A. Verl, C. Brecher, L. Uriarte and G. Pritschow, "Machine tool feed drives," *CIRP Annals - Manufacturing Technology,* vol. 60, no. 2, pp. 779-796, 2011.

[51] "ADVANCED Motion Controls," ADVANCED Motion Controls, 1987. [Online]. Available: https://www.a-m-c.com/experience/technologies/motor-type/linear/. [Accessed 28 September 2017].

[52] A. Corporation, "LE Series Linear Motor Systems". September 1999.

[53] C. Rohrig and A. Jochheim, "Identification and compensation of force ripple in linear permanent magnet motors," in *Proceedings of the 2001 American Control Conference. (Cat. No.01CH37148)*, Arlington, VA, USA, USA, 2001.

[54] J. E. Foo, S. H. Chong and S. L. Loh, "Robust tracking control of an ironless linear motor with continuous motion nominal characteristic trajectory following controller," in *2017 56th Annual Conference of the Society of Instrument and Control Engineers of Japan (SICE)*, Kanazawa, Japan, 2017.

[55] S. Chong and K. Sato, "Nominal characteristics trajectory following control as practical controller: A review," in *IECON 2015 - 41st Annual Conference of the IEEE Industrial Electronics Society*, Yokohama, Japan, 2015.

[56] J. Ko., S. Youn and Y. Kim, "A Robust Adaptive Precision Position Control of PMSM," in *Conference Record of the 2002 IEEE Industry Applications Conference. 37th IAS Annual Meeting (Cat. No.02CH37344)*, Pittsburgh, PA, USA, USA, 2002.

[57] F. Filicori, C. Lo Bianco and A. Tonielli, "Modeling and control strategies for a variable reluctance direct-drive motor," *IEEE Transactions on Industrial Electronics,* vol. 40, no. 1, pp. 105-115, 1993.

[58] L. Shihua and L. Zhigang, "Adaptive Speed Control for Permanent-Magnet Synchronous Motor System With Variations of Load Inertia," in *IEEE Transactions on Industrial Electronics*, 2009.

[59] C. C. S., "The Feedforward Friction Compensation of Linear Motor Using Genetic Learning Algorithm," in *17th IFAC World Congress (IFAC'08)*, Taipei, Taiwan, 2008.

[60] H. Olsson, K. J. Åström, C. C. d. Wit, M. Gäfvert and P. Lischinsky, "Friction Models and Friction Compensation," *European Journal of Control,* vol. 4, no. 3, pp. 176-195, 1998.

[61] H. Stampfli, "Linear motor applications: Ironcore versus Ironless Solutions," HST-Etel Inc., 2003.

[62] H. Stearns, B. Fine and M. Tomizuka, "Iterative Identification of Feedforward Controllers for Iterative Learning Control," *IFAC Proceedings Volumes,* vol. 42, no. 16, pp. 203-208, 2009.

[63] K. Sato, M. Katori and A. Shimokohbe, "Ultrahigh-Acceleration Moving-Permanent-Magnet Linear Synchronous Motor With a Long Working Range," *IEEE/ASME Transactions on Mechatronics,* vol. 18, no. 1, pp. 307-315, 2013.

[64] T.-H. Liu, H.-T. Pu and C.-K. Lin, "Implementation of an adaptive position control system of a permanent-magnet synchronous motor and its application," in *IET Electric Power Applications*, 2010.

[65] M. Zhiqiang , S. Guanghui , C. Zhihao and L. Zhengkai , "Linear motor motion control using fractional order sliding mode controller with friction compensation," in *2017 36th Chinese Control Conference (CCC)*, Dalian, China, 2017.

[66] K. S. , I. M. and O. K. , "Disturbance observer-based motion control of direct drive motors," in *IEEE Transactions on Energy Conversion*, 1991.

[67] Malek, M, Makys, P and Stulrajter, M, "Feedforward Control of Electrical Drives - Rules and Limits," *Power engineering and electrical engineering,* vol. 9, pp. 35-42, 2011.

[68] Shrot, A. and Bäker, M., "A Study of Non-uniqueness During the Inverse Identification of Material Parameters," *Procedia CIRP,* vol. 1, no. 1, pp. 72-77, 2012.

[69] Faanes, A. and Skogestad, S., "Feedforward Control under the Presence of Uncertainty," *European Journal of Control,* vol. 10, no. 1, pp. 30-46, 2004.

[70] Itagaki, H., Tsutsumi, M. and Iwanaka, H., "Design Method for High-gain Control of Linear Motor Feed Drive Systems Using Virtual Linear Friction," *Procedia CIRP,* vol. 1, no. 1, pp. 244-249, 2012.

[71] R. Vilanova, "Feedforward Control for uncertain systems . Internal Model Control approach," 2007.

APPENDICES

APPENDIX A

Positioning Performance Of CM-NCTF Controller Compared with PTOS Controller

Table A-1: Transient analysis of CM-NCTF and PTOS for 10 times repeatability in different step height

Step Height (mm)	Performance index	Controller	
		CMNCTF	PTOS
0.1	T_{rise}, s	2.04×10^{-2}	9.60×10^{-2}
	T_{settle}, s	8.90×10^{-2}	N/A
	%OS, %	0	0
	SSE, µm	0	7
1	T_{rise}, s	7.20×10^{-2}	8.10×10^{-2}
	T_{settle}, s	9.60×10^{-2}	1.30×10^{-1}
	%OS, %	0	0
	SSE, µm	0	7.66
10	T_{rise}, s	2.30×10^{-1}	1.4×10^{-1}
	T_{settle}, s	3.10×10^{-1}	2.20×10^{-1}
	%OS, %	0	0
	SSE, µm	0	6.94
50	T_{rise}, s	7.10×10^{-1}	2.80×10^{-1}
	T_{settle}, s	9.40×10^{-1}	4.1×10^{-1}
	%OS, %	0	0
	SSE, µm	0	9.88

*N/A denotes not available

Table A-2: Maximum error and root-mean-square error of CM-NCTF and PTOS for 10 times repeatability in tracking motion

Freq. (Hz)	Amplitude (mm)	Controller	e_{max} (μm)		e_{rms} (μm)	
			Average	Standard Deviation	Average	Standard Deviation
0.1	0.1	CM-NCTF	1.73	4.11×10^{-2}	4.06×10^{-1}	2.13×10^{-3}
		PTOS	3.62×10^{1}	9.72×10^{-1}	2.80×10^{1}	5.05×10^{-1}
	1	CM-NCTF	4.68	1.44×10^{-1}	1.10	6.8×10^{-3}
		PTOS	4.59×10^{1}	5.58×10^{-1}	3.60×10^{1}	1.79×10^{-1}
	50	CM-NCTF	1.51×10^{1}	8.12×10^{-1}	2.92	3.11×10^{-2}
		PTOS	3.67×10^{2}	1.59	2.47×10^{2}	5.28×10^{-1}
1	0.1	CM-NCTF	6.16	8.89×10^{-2}	2.41	1.04×10^{-2}
		PTOS	3.87×10^{1}	4.13×10^{-1}	2.96×10^{1}	1.93×10^{-1}
	1	CM-NCTF	9.97	2.44×10^{-1}	3.57	4.41×10^{-2}
		PTOS	8.83×10^{1}	4.39×10^{-1}	6.71×10^{1}	1.77×10^{-1}
	50	CM-NCTF	2.04×10^{1}	6.33×10^{-1}	7.79	2.93×10^{-2}
		PTOS	7.68×10^{3}	3.07	4.91×10^{3}	4.76×10^{-1}
1.5	50	CM-NCTF	3.77×10^{1}	1.16	2.09×10^{1}	1.62×10^{-1}
		PTOS	1.46×10^{4}	3.04	9.61×10^{3}	6.10×10^{-1}
3	1	CM-NCTF	1.20×10^{1}	3.90×10^{-1}	4.92	7.03×10^{-2}
		PTOS	1.28×10^{2}	1.36	8.61×10^{1}	9.93×10^{-2}
	5	CM-NCTF	1.95×10^{1}	1.94×10^{-1}	9.91	3.03×10^{-2}
		PTOS	9.97×10^{2}	9.16×10^{-1}	7.02×10^{2}	1.71×10^{-1}
5	0.1	CM-NCTF	8.50	2.65×10^{-1}	4.07	1.05×10^{-1}
		PTOS	5.86×10^{1}	2.62×10^{-1}	4.02×10^{1}	2.97×10^{-2}
	1	CM-NCTF	1.54×10^{1}	6.83×10^{-1}	7.30	1.09×10^{-1}
		PTOS	3.39×10^{2}	1.12	2.28×10^{2}	3.96×10^{-1}
	5	CM-NCTF	7.90×10^{1}	5.60×10^{-1}	4.85×10^{1}	2.47×10^{-1}
		PTOS	1.98×10^{3}	1.55	1.36×10^{3}	2.13×10^{-1}

APPENDIX B

Table B: Specifications of linear motor (IPMLM)

Parameters	Values	Units
Continuous Force	75	N
Continuous Current	2.3	A
Peak Force	225	N
Peak Current	6.9	A
Grating Resolution	0.1	µm
Effective Stroke	155	mm
Positioning accuracy	1	µm
Maximum Speed	1	m/s
Maximum Acceleration	10	F
Maximum Load	8	kg
Dimensions	140 x 400 x 75	mm
Weight	8.0	kg

APPENDIX C

Table C: Pin connection of direct drive system to Microbox

CN1 (Female)			
Pin	**Abbr.**	**Description**	**Microbox**
1	A0+	Encoder Channel A+	Not in Use
3	OUT	Analog Output	Con 2, Pin 11 (DAC)
21	GND	Ground	Con 2, Pin 19/20 (DAC)
42	VCC	VCC	Con 3, Pin 16 (ENC)
43	B0+	Encoder Channel B+	Not in Use
62	GND	Ground	Con 3, Pin 19/20
CN2 (Male)			
Pin	**Abbr.**	**Description**	**Microbox**
1	SON	Servo On	Con 1, Pin 1 (DIO)
5	HOME	Home Limit Switch	Not in Use (DIO)
23	CLEAR	Clear Axis	Not in Use (DIO)
27	LM0+	Positive Limit Switch	Not in Use (DIO)
41	GND	Ground	Con 1, Pin 18 - 20
45	ALARM	Alarm	Not in Use (DIO)
48	LM0-	Negative Limit Switch	Not in Use (DIO)

APPENDIX D

Expected Results

From the Figure D-1, it shows that the continuous-motion nominal characteristics trajectory following (CM-NCTF) do not have any steady-state error and overshoot occurrence at the point-to-point (PTP) motion. However, from the Table D-1, the analysis shows the slower transient response on the motion performance. In Figure D-3, the CM-NCTF controller has a low tracking performance at high frequency motion. Thus, the next experiment will focus on the fast response at PTP motion by reducing the rise time and settling time to improve the motion performance in terms of PTP and tracking motion. In the research [29], the author has used the CM-NCTF controller with velocity feedforward compensator to improve the tracking performance as shown in Figure D-4. In this research, CM-NCTF controller with and without velocity feedforward element is used to examined using an AC driven X-Y ball screw mechanism. As a result, the CM-NCTF with velocity feedforward has shown the less effect on the variation of the sinusoidal input and give a smallest motion error compared to the controller with only the CM-NCTF as shown in Table D-3. Besides, it also showed that the CM-NCTF with velocity feedforward controller has a fast response on the tracking performance. Therefore, the CM-NCTF with velocity feedforward controller do show the potential to reduce the motion error and may achieve a fast response on both point-to-point and tracking motion.
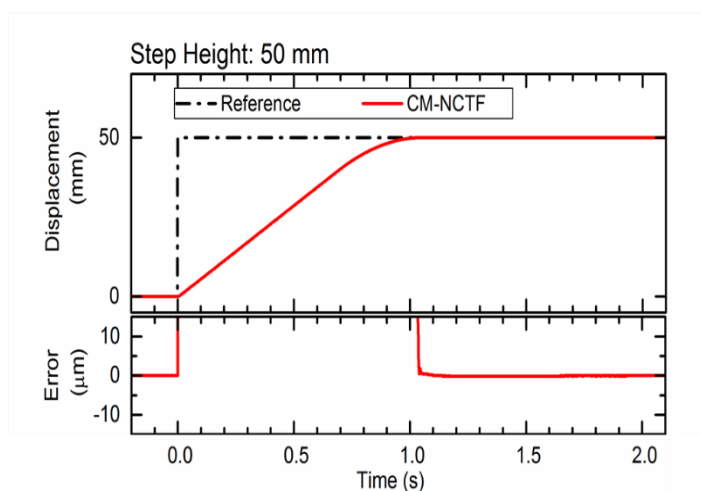
Figure D-1: Experimental PTP response of CM-NCTF controller at 50-mm step height [14]

Table D-1: Transient analysis of CM-NCTF at 50-mm step height in PTP motion [14]

Rise time, $t_r(s)$	0.71
Settling time, $t_s(s)$	0.94
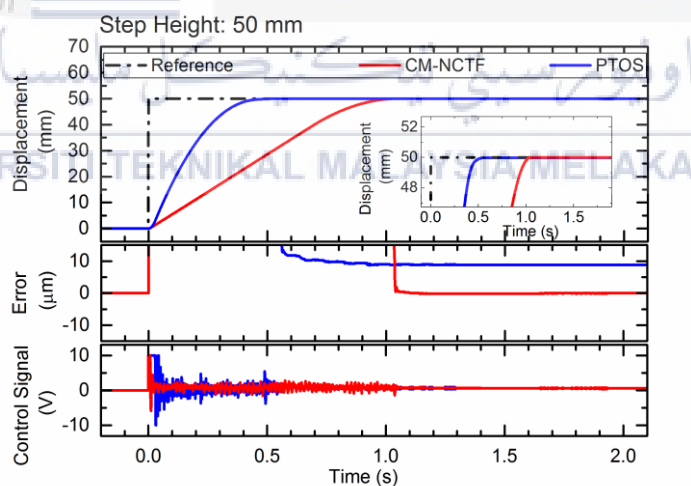
Figure D-2: Comparative PTP response of CM-NCTF and PTOS controller at 50-mm step height [14]

Table D-2: Maximum error, E_{max} of the CM-NCTF controller in tracking motion [14]

Amplitude (mm)	Frequency (Hz)	Maximum error, E_{max} (µm)
5	3	19.5
	5	79.0
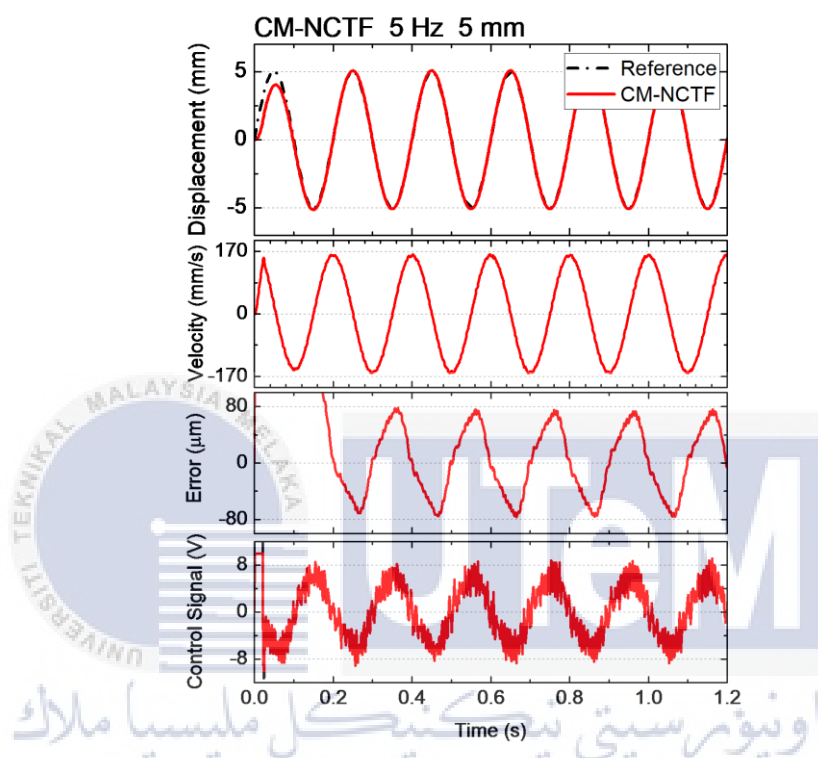
Figure D-3: Tracking response of CM-NCTF for sinusoidal input of 5 mm, 5 Hz [14]

Table D-3: Maximum error, E_{max} of the CM-NCTF controller with and without velocity feedforward compensator [29]

Frequency (Hz)	Amplitude (mm)	Maximum error, E_{max} (µm)	
		CM-NCTF controller only	CM-NCTF controller with velocity feedforward compensator
5	1	105	30
	10	1592	475
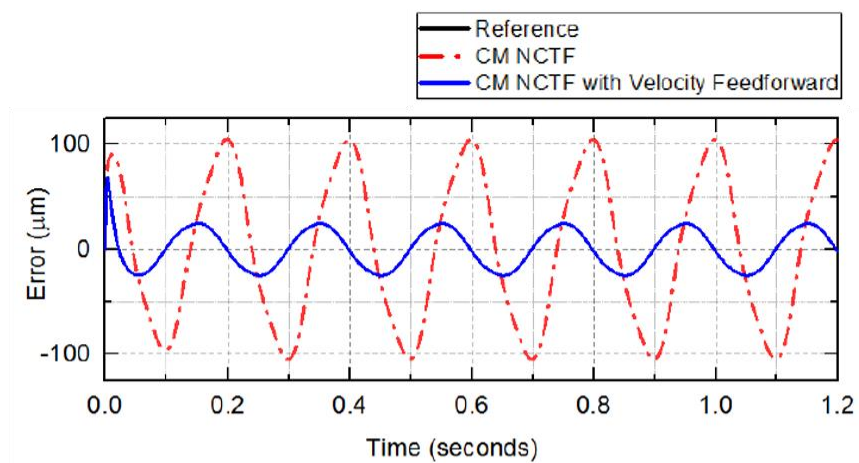
(a)
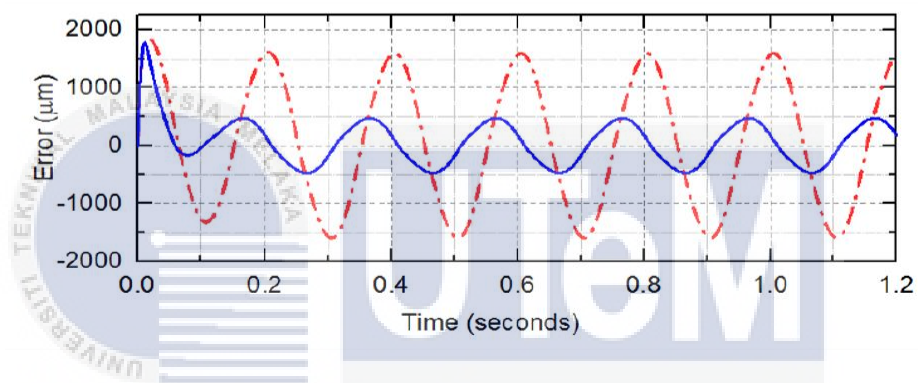
(b)

Figure D-4: Simulation result of CM-NCTF controller with and without velocity feedforward using frequency of 5 Hz at the amplitude of: (a) 1 mm, and (b) 10 mm

[29]

APPENDIX E

Project Gantt Chart

No.	Project Description/Task	Week 1	2	3	4	5	6	7	8	9	10	11	12	13	14
	YEAR 2017 (semester 1)														
1	Title Selection and Submission	▓	▓												
2	Project Introduction and Briefing		▓	▓											
3	Papers Research and Studies				▓	▓	▓	▓	▓	▓					
4	Progress Meeting of FYP 1			▓	▓		▓			▓	▓	▓			
5	Mathematical Modelling				▓	▓	▓	▓	▓						
6	Experiment Setup and Analysis									▓	▓				
7	Report Writing 1								▓	▓	▓	▓	▓		
8	FYP 1 Seminar												▓		
9	FYP 1 Report Submission													▓	▓
	YEAR 2018 (semester 2)														
1	Progress Meeting of FYP 2				▓		▓		▓	▓					
2	Controller Design				▓	▓									
3	Baseline Study	▓	▓	▓	▓	▓									
4	Validation of System Performance						▓	▓	▓	▓					
5	Report Writing 2						▓	▓	▓	▓	▓	▓	▓		
6	FYP 2 Seminar												▓	▓	
7	FYP 2 Full Report Submission													▓	▓